Calibration and Model Uncertainty of a Two-Factor Mean-Reverting Diffusion Model for Commodity Prices

by

Jue Jun Chuah

A thesis

presented to the University of Waterloo

in fulfillment of the

thesis requirement for the degree of

Master of Quantitative Finance

Waterloo, Ontario, Canada, 2013

I hereby declare that I am the sole author of this thesis. This is a true copy of the thesis, including any required final revisions, as accepted by my examiners.

I understand that my thesis may be made electronically available to the public.

Abstract

With the development of various derivative instruments and index products, commodities have become a distinct asset class which can offer enhanced diversification benefits to the traditional asset allocation of stocks and bonds. In this thesis, we begin by discussing some of the key properties of commodity markets which distinguish them from bond and stock markets. Then, we consider the informational role of commodity futures markets. Since commodity prices exhibit mean-reverting behaviour, we will also review several mean-reversion models which are commonly used to capture and describe the dynamics of commodity prices. In Chapter 4, we focus on discussing a two-factor mean-reverting model proposed by Hikspoors and Jaimungal, as a means of providing additional degree of randomness to the long-run mean level. They have also suggested a method to extract the implied market prices of risk, after estimating both the risk-neutral and real-world parameters from the calibration procedure. Given the usefulness of this model, we are motivated to investigate the robustness of this calibration process by applying the methodology to simulated data. The capability to produce stable and accurate parameter estimates will be assessed by selecting various initial guesses for the optimization process. Our results show that the calibration method had a lot of difficulties in estimating the volatility and correlation parameters of the model. Moreover, we demonstrate that multiple solutions obtained from the calibration process would lead to model uncertainty in extracting the implied market prices of risk. Finally, by using historical crude oil data from the same time period, we can compare our calibration results with those obtained by Hikspoors and Jaimungal.

Acknowledgements

To Cecilia Liu, my family and friends who have supported me in the process

Contents

List of Tables

List of Figures

Chapter 1

Introduction

For a long time, commodities were viewed as consumption assets that were either consumed or used as production inputs to generate refined goods, such as wheat for bread, crude oil for gasoline, copper for electrical wire, and etc. In the beginning, the commodity markets started off with the trading of agricultural products like corn and cattle. With the advancement of human civilization, the scope of commodities has grown to include metals and energy. Trading in commodity markets has also evolved significantly from the days when in the absence of money, barter systems were organized at town marketplaces to exchange goods. Forward agreements were then established between producers and merchants as pledges to make certain transactions at future dates. In the 17$^{\text{th}}$ century, the Dojima Rice Exchange in Osaka, Japan constituted the world's first organized futures market with standardized contracts and clearing houses guaranteeing the creditworthiness of transactions. At that time, rice was used as the basic unit of account for financial purposes and hence the Dojima futures market played an important role in the economy by providing price discovery and price stability in the rice

market. Today, producers and users of commodity products can use a wide range of more complex commodity derivatives (e.g. options, swaps, swaptions and spread options) to mitigate their risk.

The historically low interest rates environment and sluggish stock market performance in recent years, along with the development of various commodity derivatives and commodity index products, have helped to turn commodities into an alternative investable asset class, which could be a part of the strategic asset allocation in one's portfolio. Over the last decade, a huge demand from China and other emerging markets for energy and industrial metals to support their manufacturing and infrastructure development has driven the prices of commodities higher and made them an attractive asset class with superior returns. An increasing number of pension funds and sovereign wealth funds are allocating more investments into commodities as a protection against the risk of rising inflation and to further diversify their allocation beyond the tradition asset classes – stocks, bonds and cash. Since commodities are directly linked to the components of inflation, any deviations from the expected inflation level should be reflected in the price movements of commodities. Therefore commodities, like crude oil and gold, are a useful hedge against the risk of rising price levels. On the contrary, nominal bond yields are priced to compensate investors for expected inflation over the course of holding the bond. Any deviations from the expected inflation will then erode the real purchasing power of the investor. When the general price level rises dramatically, businesses will have to pay more for wages and raw materials. In the short run, this will bring down the profitability of businesses and will negatively impact their stock's performance. On the other hand, commodity spot prices and commodity futures prices

have historically outpaced inflation. Commodities as a distinct asset class can also offer enhanced diversification benefits to traditional asset allocation because of their low or negative correlation to stocks and bonds. According to Gorton and Rouwenhorst (2005), commodities tend to perform well during the early stage of a recession when stocks and bonds returns are generally disappointing. Commodities, especially precious metals, have traditionally been perceived as a "safe haven" to hedge against the event risk during periods of stress and uncertainty in the economies or politics. For example, during the Persian Gulf War, the average prices of crude oil doubled while equities faltered. Some commodities can also be used as a means of preserving value during a fiat currency crisis. Since most commodities are priced in US dollars, devaluation of the currency will drive commodity prices up. To better demonstrate the effects of adding commodities in a strategic asset allocation, we can compare the efficient frontiers of two portfolios with and without commodities. For the purpose of creating the efficient frontiers, we used the Barclays Capital U.S. Aggregate Bond Index (formerly the Lehman Aggregate Bond Index) to represent the performance of bond investments during the period of January 1987 to the end of 2007. The performance of equities investments was described by the Standard and Poor's 500 Total Return Index. In addition, we chose the Gorton and Rouwenhorst Commodity (GRC) Index as the proxy for commodities' performance during the same time period. The GRC Index is an equally-weighted collateralized commodity futures index that includes every commodity futures contract traded in the U.S. and the London Metal Exchange. The index is reweighted monthly with an equal weight given to each contract. We obtained the monthly returns data for the bond and stock market indices from a database maintained by the International Traders Research Inc., while the data for the GRC Index is obtained from the National Bureau of Economic

Research's website.[1] Figure 1.1 shows these efficient frontiers constructed using historical data over the period of 01/01/1987 to 31/12/2007. It is rather obvious that by including commodities in the strategic asset allocation, the risk-return tradeoff was improved and the resultant efficient frontier dominated that without any investment in commodities. From 1987 to 2007, the average improvement in historical annualized return for a given risk level was roughly 111 basis points with a maximum improvement of 160 basis points.
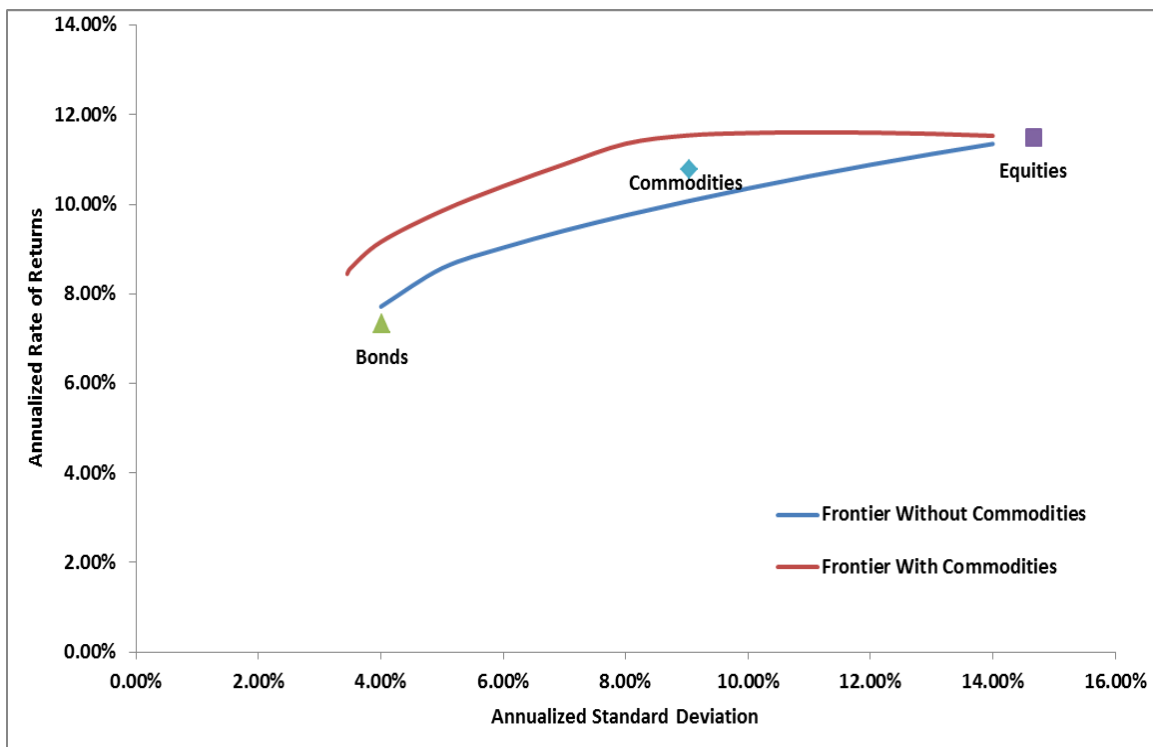
Figure 1.1: Efficient frontiers with and without commodities

At this point, we should certainly recognize commodities as an asset class in its own right. However, there are some fundamental differences between commodities and other conventional asset classes, like stocks and bonds. First of all, commodities cannot

---

[1] www.nber.org/data-appendix/w10595

be priced by the net present value of the expected future cash flows. The financial purpose of bonds and stocks is to raise external capital for the issuer. Investors are then compensated for the time value of the money put upfront and for the risk of possible low future cash flows. Therefore, a bond is valued by its discounted expectation of future coupon and principal payments, while a stock is priced with dividend payments and/or share repurchases as future cash flows. On the other hand, commodities are not capital assets but rather resources primarily used as inputs in production processes to generate refined goods. Hence, commodity spot prices are determined by the intersection of their supply and demand curves. Besides that, some commodities also exhibit noticeable seasonality in their price levels and volatilities, due to changes in supply and demand, in fairly consistent patterns. To illustrate the seasonality in commodity prices, we obtained the historical spot prices of lean hogs from a database maintained by the Commodity Systems Inc. (CSI). The CSI database contains daily spot and futures prices for over hundreds of commodity markets worldwide. This database will be used as the primary data source to conduct all studies in this thesis here onwards unless stated otherwise. From Figure 1.2, strong seasonality can be observed in the lean hogs market. The price of lean hogs has a tendency to move higher from early March until July as inventories drop ahead of summer grilling season.

Given the differences stated above, commodities should be perceived as a distinct asset class, and, when it comes to pricing commodities derivatives, they should be treated differently from other conventional asset classes. In Chapter 2, we subsequently consider the informational role of commodity futures markets. Since commodity prices exhibit mean-reverting behaviour, we will review several mean-reversion models that are
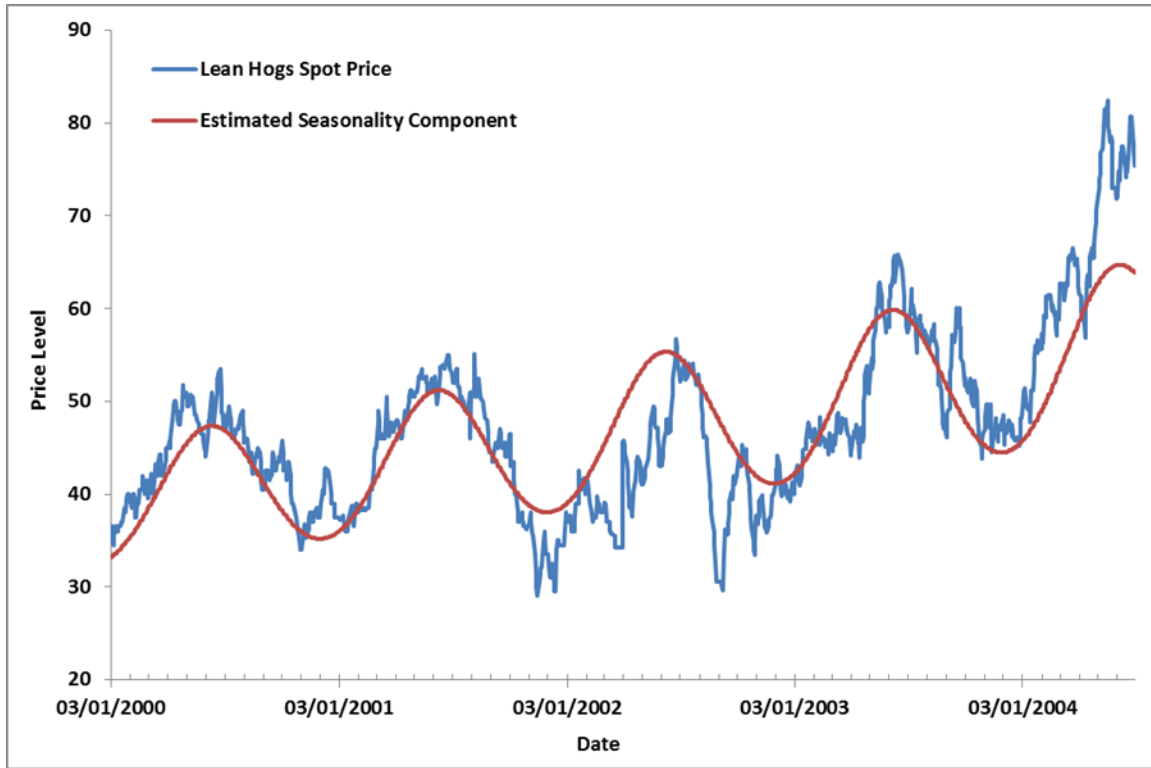
Figure 1.2 Lean hogs spot price and its estimated seasonality component[2]

commonly used to describe the dynamics of commodity prices in Chapter 3. In Chapter 4,

we discuss a two-factor mean-reverting model proposed by Hikspoors and Jaimungal, as

a means of providing additional degree of randomness to the long-run mean level. They

also suggested a method to extract the implied market prices of risk, after estimating both

the risk-neutral and real-world parameters from the calibration procedure. The usefulness

of this model motivates us to investigate the robustness of this calibration process by

applying the methodology to simulated data. In Chapter 5, the capability to produce

stable and accurate parameter estimates will be assessed by selecting various initial

guesses for the optimization process. When multiple solutions are provided by the

---

[2] The seasonality term, g_t, is described by the function $g_t = C + A_0 t + A_1 \sin(2\pi t) + B_1 \cos(2\pi t)$ where C is the intercept at time $t = 0$.

calibration method, we further show the presence of model uncertainty in the calculation of market prices of risk. Finally, we compare our calibration results with those obtained by Hikspoors and Jaimungal by using historical crude oil data from the same time period.

Chapter 2

Commodity Futures Contracts

There are several ways an investor or a hedger can gain exposure to the price movements of a commodity. Investors or hedgers can choose to take positions in the physical commodity by carrying out transactions in the spot market with producers or intermediaries. However, they have to deal with the issues of transporting and storing the physical commodity. This can be a costly process for investors to profit from the price movements of commodities or for hedgers to mitigate their price risk. Buying the stocks of commodity-related companies can also be a way of benefiting from the anticipated rise in commodity prices. By doing so, investors are also exposed to the idiosyncratic risk that is unique to the company. Poor corporate governance and geopolitical risk (i.e. government intervention) can have major effects on the stocks' performance. The exposure to potential upsides in commodity prices is also limited by the fact that companies are practicing risk management activities to smooth out their earnings over time. In year 2011, there was an apparent disconnection between gold prices and the stocks of gold mining companies. The spot gold price had risen about 11% for the year,

but mining stocks in the S&P/TSX Global Gold Index declined more than 14% in the same time period due to the rising cost of mining the precious metal. Most commodity-related equities have positive betas to the stock market as a whole. This makes commodity-related equities less effective in diversifying a strategic asset allocation.

With the creation of futures contracts, investors or hedgers have a more direct way to build targeted exposure to commodities. A futures contract is a standardized agreement struck between two parties to exchange at a specified future date a standardized quantity and quality of a commodity for a price agreed today. These contracts are traded on a futures exchange such as the Chicago Mercantile Exchange (CME) and the London Metal Exchange (LME) with clearing houses standing behind the exchange to deal with both the buyers and sellers of the futures. By having a clearing house acting as an intermediary between buyers and sellers, any counterparty risk from the two participants engaged in the transaction is essentially taken away. Additionally, investors or hedgers can attain a leverage effect through the trading of futures contracts since they are only required to pay upfront a margin deposit which is a small fraction of the futures contract's face value. Futures contracts also provide market participants the flexibility of going long or short the contract, hence the choice of a positive or negative exposure to a rise in commodity prices. A buyer and a seller of a futures contract can choose either to go into physical delivery of the commodity at maturity or to terminate the position prior to settlement by taking a symmetric position in the futures contract with the same maturity in order to nullify the position. The ability to close out a position by taking the opposite position enables investors and hedgers to avoid the cumbersome and costly procedure of physical delivery. According to the CME, only a small percentage of

the futures contracts are held to settlement and are obligated to make physical delivery. Given the price transparency and liquidity provided by futures contracts, they appear to be an ideal and cost-efficient way for investors and hedgers to gain exposure to commodities. Hedge funds and Commodity Trading Advisors (CTA) are using futures contracts as a substitute for the spot market to gain access to commodities.

2.1 Hedging with Futures and Basis Risk

From the start, a commodity futures contract was designed to meet the needs of hedgers to mitigate their exposure to price risk. Today, futures contracts are still widely used by producers and commodities users to lock in their prices in advance. For instance, an airline company that wants to reduce its exposure to volatile and possibly rising fuel prices will buy futures contracts in crude oil to hedge against the risk. A farmer who anticipates a forthcoming oversupply of corn might want to sell corn futures to lock in the prices for his harvest. However, when hedgers are using futures contracts to eliminate price risk, they should be aware of the basis risk that exists in the hedging practice. Basis is defined as the difference between the futures price and the spot price and can be written as:

$$Basis_{t,T} = Spot\ price_t - F^T(t)$$

where $F^T(t)$ is the price at time t of a futures contract with maturity T. Since the buyer of a futures contract may immediately sell the commodity in the spot market after taking delivery at maturity, the no arbitrage condition between the spot and futures markets implies that:

$$Spot\ price_T = F^T(T)$$

whereby the futures price should converge to the spot price at maturity. In the case where a hedger decides to terminate his futures position prematurely, he will be exposed to the basis risk we mentioned above. When the time horizon of a hedging position is different from the maturities of all available futures contracts, the position should be set up such that the basis is as small as possible. Basis risk also exists when the underlying of the futures contract is similar but not identical to the source of risk meant to be hedged. For example, an airline company that wants to hedge its exposure to rising jet fuel prices can only do so by buying either the crude oil futures or the heating oil futures since there is no futures contract on jet fuel. However, this hedging practice is subject to basis risk when the futures price of heating oil does not change by the same amount over time as that of the spot price of jet fuel resulting in non-convergence of the two prices at maturity. Therefore, basis risk refers to the risk remaining after putting on the hedge and can be measured by the variance of the basis as follows:

$$\sigma^2\big(S_t - F^T(t)\big) = \sigma^2(S_t) + \sigma^2\big(F^T(t)\big) - 2\rho\sigma(S_t)\sigma(F^T(t))$$

where ρ is the correlation coefficient between the spot and the futures prices. This equation shows that basis risk depends highly on the degree of correlation between spot and futures prices, and futures contracts that are highly correlated to the spot position should be chosen for hedging purposes. To gauge the effectiveness of hedging a spot position with futures contracts, Geman (2005) suggested the following measurement:

$$h = 1 - \frac{\sigma^2(Basis)}{\sigma^2(Spot_t)}.$$

11

From this equation, one can speculate that a hedger will be more certain about the outcomes of his hedging position when the variance of basis is small. Subsequently, a hedge will be more effective when h is closer to 1. Going back to the previous example we have, if both the crude oil and heating oil futures are available to hedge the price risk of jet fuel, the airline company should choose the contract that leads to a higher value of h.

2.2 Informational Role of Futures Markets

Given the lack of liquidity in both the spot and forward markets, one of the important roles of futures markets is to provide price discovery in the commodity market. A variety of market participants (such as hedgers and speculators) interact on the futures exchanges to bring liquidity and price transparency to the marketplace. No arbitrage conditions between the spot and futures markets can also be maintained with the presence of arbitrageurs to quickly absorb any price abnormalities that appear between the two markets. Futures prices are determined through competitive and transparent trading on the exchange to reflect the supply and demand of the underlying and the traders' expectation of spot prices at various time points in the future. Hence, the informational content of the futures curve, i.e., the set of all available futures prices as a function of their maturity, is of particular interest to all agents in the economy. One of the important social utilities offered by the futures markets is the forecasting power of futures curve to predict the future spot prices which directly affects the effectiveness of using futures contracts in hedging activities. The fact that one can make better speculations about future spot prices based on the current future curve allows companies to more accurately assess the future supply and demand, which can benefit the decision making process on

production, consumption and storage of commodities. The price discovery process in futures markets helps companies to mark-to-market their positions in a trading book without relying on the view of a specific trader. In his influential article, Grossman (1977) stressed the informational role of futures markets. He argued that futures markets serve the role as a marketplace where information is exchanged and market participants collect and analyse information about future states of the world to earn a return on their investment. According to Grossman, information about the future spot prices is transmitted at the futures markets from the "informed" traders to the "uninformed" traders.

2.3 Theory of Storage and Convenience Yield

Over the past decades, some economists have tried to explain the differences between spot and futures prices with the theory of storage. By investigating the reasons why economic agents hold inventories, these models stress the importance of knowing the quantities produced and the storage level in deriving the term structure of storable commodities. For storable commodities, the futures price acts as a measure of inventory allocation. In contrast, the futures market serves as a source of price stability for non-storable commodities such as lean hogs, live cattle, and electricity. Since commodities are mostly used as inputs in production, holding the physical commodity as inventory allows us to meet unexpected demand and to avoid any disruption in production in the event of a supply shortage. Kaldor (1939) and Working (1948, 1949) propose the notion of convenience yield as the advantages associated with physical owning the commodity. The owner of physical commodity enjoys the benefit of conveniently gaining access to the asset when needed, which is not obtained from holding the futures contract. In

principle, this may be viewed as analogous to the dividend yield for a stock, where a dividend is paid to the shareholder while the holder of a derivative contract written on the stock will not receive the distribution. Some economists also view convenience yield as a timing option embedded to physically owning the commodity. Brennan (1958) and Telser (1958) argue that owner of the physical commodity keeps an option between selling the commodity in the market when prices are high and holding it for future utilization when prices are low.

The convenience yield, y, is defined as the present value of the benefit of holding the physical commodity minus the present value of the cost paid for storing the goods. Therefore, y can take different signs depending on the inventory level, the time period, and the type of commodity. Routledge, Seppi and Spatt (2000) suggest that the convenience yield is inversely related to the level of inventories, as the gain from holding the physical commodity will be high when inventories are low. The different values of convenience yield can also help us to account for the various shapes of futures curves, such as contango and backwardation, which will be further explained in Section 2.5. Given the importance in explaining the different shapes of futures curves, many studies have chosen to introduce the convenience yield as an additional state variable to improve the quality of modeling the price process dynamics. Gibson and Schwartz (1990) first introduced a two-factor model with the convenience yield that follows a mean-reverting stochastic process. On the contrary, Routledge et al proposed an equilibrium model for storable commodities, such that convenience yield is an endogenous variable that depends on the storage process. The authors developed a model for which predictions about the volatilities of forward prices are able to be made at different time horizons.

Other than explaining the different shapes in futures curves, the level of storage also has great influence on the volatility of commodity prices. By studying the behaviour of futures prices for metals, wood and animal products, Fama and French (1987) conclude that the standard deviation of prices increases when the level of inventory is low. A more recent study by Geman and Nguyen (2005) on the worldwide soybean inventories over a 10-year period shows that price volatility can be written as an inverse function of inventory. When the market is experiencing a supply or a demand shock, inventories can be used as buffers to absorb any changes to the supply and demand curves, so that changes to the commodity prices will be less dramatic. At the same time, low inventory levels normally coincide with high commodity prices, and hence there exists a strong negative correlation between prices and the levels of inventory. Figure 2.1 depicts the negative correlation between the spot price of wheat and its storage level in the U.S. over a 10-year period from January 1990 to December 1999. Monthly ending stocks data for the U.S. wheat market is obtained from the United States Department of Agriculture's website.[3] We observe that the wheat price rises sharply during periods of low inventory level while the decline in price is modest in comparison since the physical stock of wheat can only be replenished gradually. Since the commodity price and its volatility are both negatively correlated to the inventory level, this implies that the price and volatility of a commodity market are positively related to each other. This phenomenon in commodity markets is in sharp contrast to the so-called "leverage effect" in the equity markets. The "leverage effect" refers to the well-established inverse relationship between stock volatility and stock returns, i.e., volatility tends to increase

---

[3] www.ers.usda.gov/data-products/wheat-data.aspx#25377
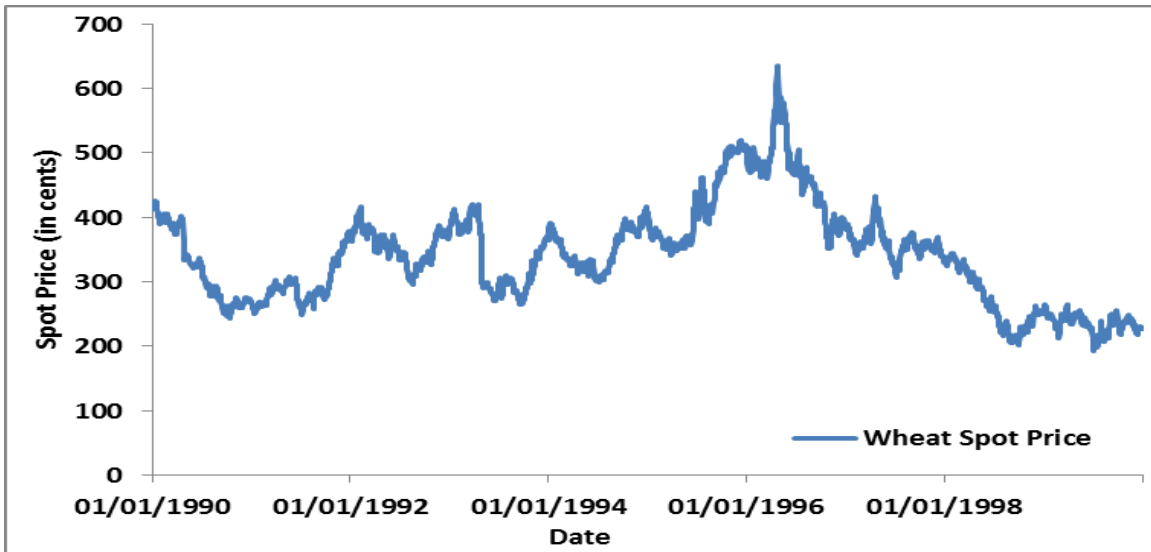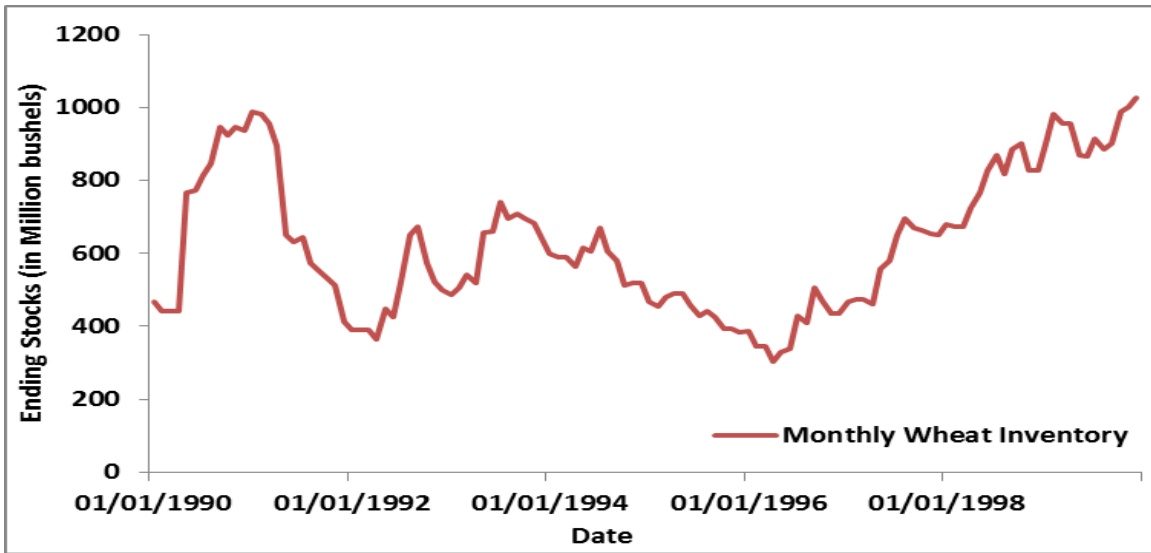
Figure 2.1 The relationship between wheat spot price and its inventory level

when stock prices fall. In his paper published in 1965, Samuelson asserts that, ceteris paribus, the volatility of futures prices tends to decrease with their time-to-maturity. This well-known property of futures curves is also known as the "Samuelson effect". The "Samuelson effect" can be explained by the fact that any shock to the demand and supply curves should have an immediate impact on the prices of short-term futures contracts

while the longer-term contracts tend to be less affected by the news since production can be adjusted to accommodate this new information before these contacts mature. Figure 2.2 presents monthly term structures of the Sugar No. 11 futures contract traded at the Intercontinental Exchange (ICE) over the period January 2007 to December 2011. The fact that the nearest-maturity contract has the largest variation in futures prices when compared to longer-term contracts reaffirms the existence of the "Samuelson effect" in the world sugar market. In the graph, we can also observe different shapes of futures curves (contango and backwardation) that appear in the sugar market. In addition to inventory level, reserves estimates also have a huge impact on price movements and
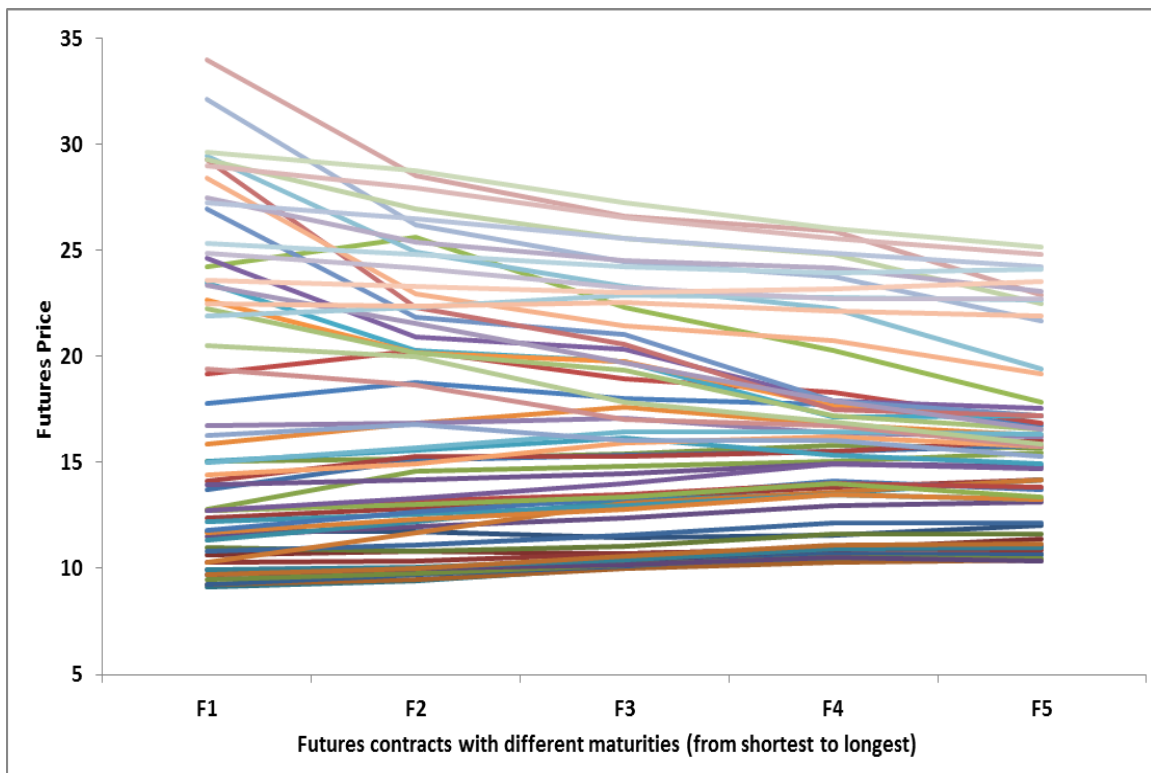
Figure 2.2 Monthly term structures of the Sugar No. 11 futures contract[4]

---

[4] Here, F1 denotes the first-nearest contract, which is the futures contract that has the shortest time-to-maturity, while F2 represents the futures with the second shortest time-to-maturity, and so on. Typically, the maturities of these contracts are 2 months, 4 months, 9 months, 12 months and 14 months.

volatilities of commodities. This phenomenon is particularly observed in the energy markets, such as crude oil and natural gas markets, where the reserves are limited and expected to be depleted after a finite amount of time, usually within decades.

2.4 Rational Expectations Hypothesis

Given the informational role of futures markets, one of the natural questions that comes to mind is whether the futures price at time t can be considered as a predictor, in some sense, of the future spot price at maturity T. In mathematical terms, we can write the statement as:

$$F^T(t) = E[S(T) \mid \mathcal{F}_t] \tag{2.1}$$

where $\mathcal{F}_t$ represents the information available in the market at time t. If equation (2.1) is satisfied, then we can consider futures price as an unbiased predictor for the unknown future spot price. Muth (1961) and Lucas (1976) put forward the Rational Expectations Hypothesis to argue that economic agents make rational predictions about future states of the economy based on available information and past experiences, and these expectations do not differ systematically from the true future values. A study performed by Frenkel (1977) on the German Mark shows that observed data from the forward market can provide rational expectations of the future exchange rate. However, for the broader commodity market, evidences from previous studies to support the hypothesis have been inconclusive and most tests conducted have led to the rejection of equation (2.1). Hence, the futures price $F^T(t)$ is considered a biased estimator of the future spot price $S(T)$, since equation (2.1) does not hold. If the future price is always higher than the expected spot price at maturity T, then $F^T(t)$ is an upward-biased estimator. This scenario can be

caused by the fact that commodity users are so eager to secure access to the commodity at maturity that they are willing to pay a premium on top of the expected spot price. In contrast, when the market is expecting an excess supply of the commodity, the futures price $F^T(t)$ might be lower than the expected spot price $S(T)$, as producers are anxiously seeking to hedge the price risk of their output.

2.5 Backwardation and Contango

Keynes (1930) and Hicks (1939) proposed the theory of normal backwardation to explain this market behaviour and stated that in order for speculators to take on risky positions in the futures markets, futures prices have to be, in general, downward-biased estimates of the future spot prices. They argue that the futures markets are primarily dominated by commodity producers who are seeking to lock in the future prices of their output and would buy protection in the futures markets to hedge against the price risk. Speculators, on the other hand, would like to provide this insurance and buy the futures provided that they receive a premium in return to compensate for the risk they have taken. Therefore, the futures price has to be set lower than the expected spot price at the maturity and the difference between these two prices represents the risk premium producers would have paid to the speculators for bearing the risk of future price fluctuations. Figure 2.3 gives us a graphical illustration of normal backwardation. Assume that the current spot price for a barrel of crude oil is $50 and the market is expecting the price to go down $5 in three months to become $45 per barrel. In order to attract speculators to take on the risk of future price fluctuations, the 3-month futures contract will be priced at $43, which is a $2 discount to the expected spot price. The two dollars difference between the 3-month futures price and the expected future spot price is the risk premium earned by speculators

for providing insurance to the hedgers. However, the theory of normal backwardation may be obsolete for current futures markets, as the theory is built on the assumption that hedgers as a whole are net short in the futures markets. This assumption is no longer
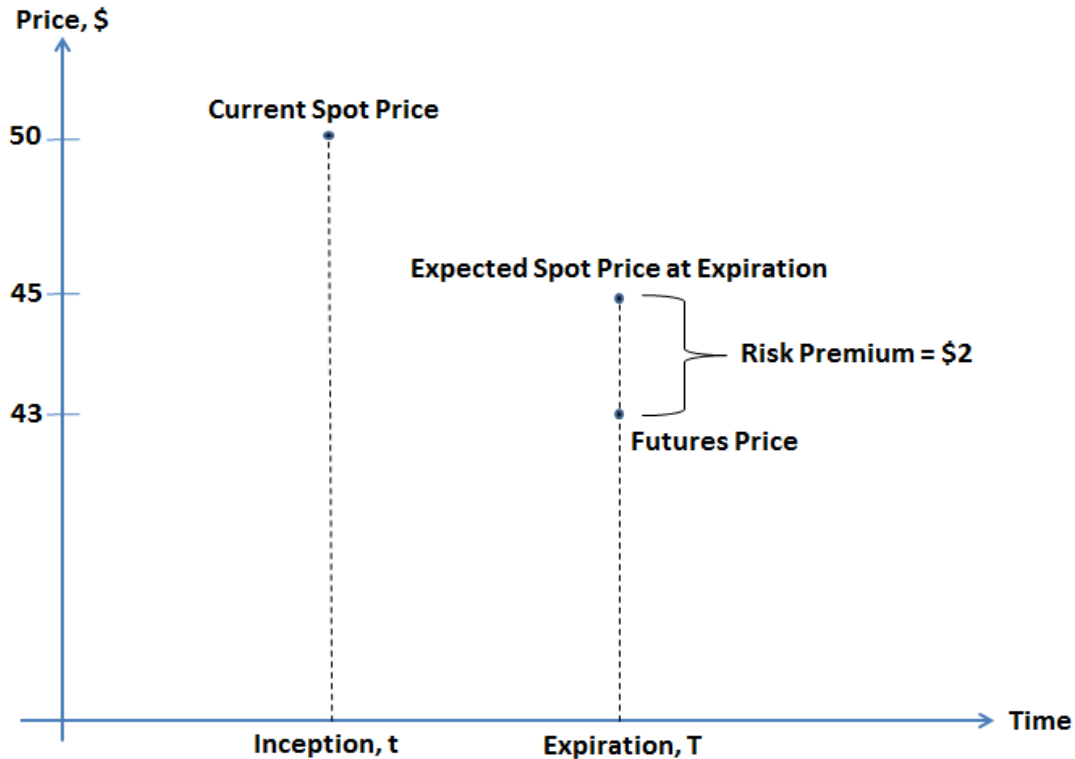
Figure 2.3 An example of normal backwardation

valid due to market evolvement from a producer-dominated futures market to the current market shared by a variety of market participants such as producers, intermediaries, and hedge funds, as well as commodity users who want to hedge the price risk of their future consumption by buying futures contracts. In certain commodity markets, the signs of risk premiums along the same futures curve can also be different depending on the futures contract's maturity. The electricity markets are known to have very volatile spot markets due to the fact that storage is not possible for electricity. Therefore, in order to avoid any

disruptions in their production, electricity consumers are willing to pay a premium on top of the expected future spot price to secure short-term delivery of power. On the other hand, utilities are ready to sell long-dated futures contracts at a discount to the expected future spot price so that they can secure financing for their physical assets and maintain smooth cash flows in the long-term. These market behaviours cause the electricity futures curves to be upward-biased at the short end while they experience normal backwardation for longer-dated contracts.

From Section 2.3, we note that the convenience yield y plays an important role in explaining the term structure of storable commodity prices. Hence, under the assumption of no arbitrage, it can be shown that futures price $F^T(t)$ is related to the spot price S_t by the following relationship:

$$F^T(t) = S_t e^{(r-y)(T-t)} \tag{2.2}$$

where r is the continuously compounded interest rate. If we further decompose convenience yield y into two components, then y becomes:

$$y = y_1 - c$$

where y_1 represents the benefit from holding the physical commodity while c denotes the cost of storage.[5] We can then re-write equation (2.2) as:

$$F^T(t) = S_t e^{(r+c-y_1)(T-t)}. \tag{2.3}$$

If the current futures price $F^T(t)$ is greater than the right-hand side of equation (2.3), then

---

[5] c is expressed as a continuously compounded rate.

an arbitrageur can take advantage of this opportunity by selling the contract in the futures market and buying the cash commodity through a loan. He or she will then carry the commodity over the interval (t, T) and deliver it against the futures when the contract expires at T. Conversely, if the current futures price $F^T(t)$ is cheaper than the right hand side of equation (2.3), a trader would buy the futures contract and open a short position in the commodity spot market at the same time. At maturity, the trader would accept delivery and use it to cover the short position in order to capitalize on this arbitrage opportunity. With the presence of arbitrageurs to absorb any price abnormalities, these arbitrage opportunities should disappear quickly and equation (2.3) should hold under the arbitrage-free assumption.

From equation (2.3), we notice that when the benefit from holding the physical commodity, y_1, is greater than the sum of interest rate and storage cost (i.e., $y_1 > r + c$), this will result in a downward-sloping term structure and we will have a situation of backwardation:
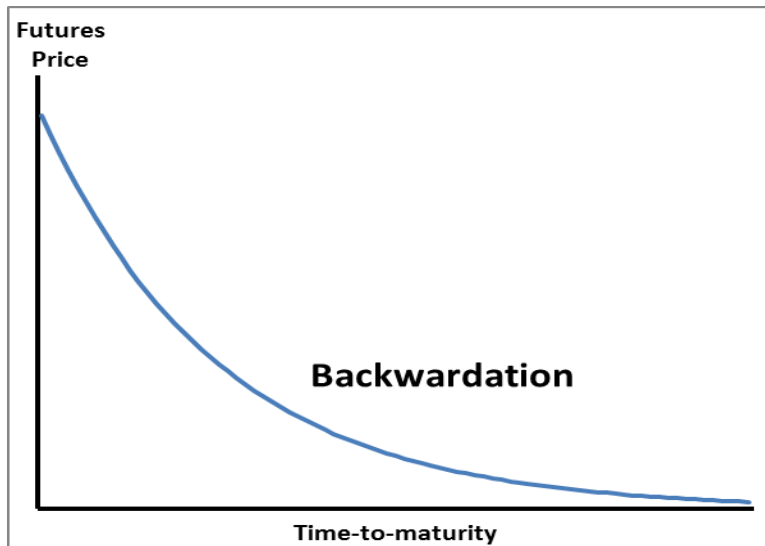
Figure 2.4 An illustration of backwardated futures curve

Normally, backwardated term structures can be observed when convenience yields are positive and high during periods of tight supply in a commodity. Conversely, when benefits of physical ownership of a commodity are low relative to the interest rate and storage costs (i.e., $y_1 < r + c$), the commodity term structure will be upward sloping and the futures market is in contango:
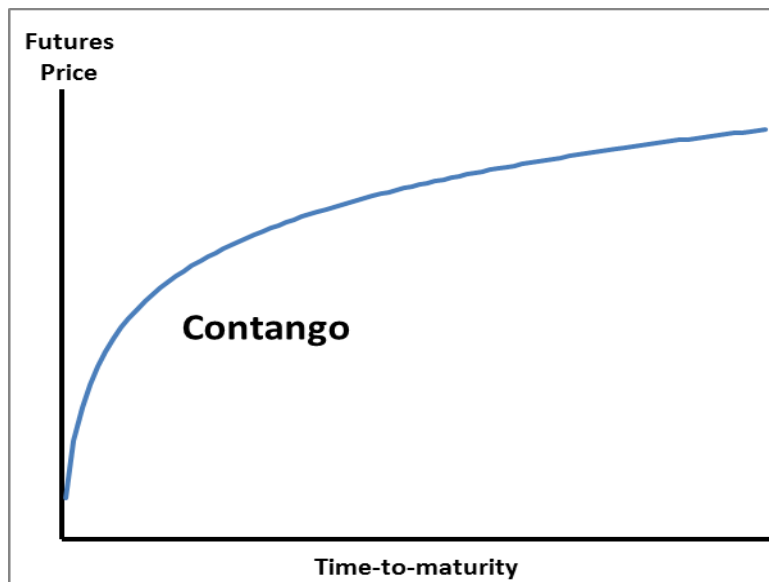
Figure 2.5 An illustration of futures curve in contango

Hence, convenience yield is essential in determining the shapes of futures curves. However, we should note that the spot-futures relationship stated in equation (2.2) is based on the assumption that both the interest rate *r* and convenience yield *y* are constant over the futures contract's holding period. This assumption may be true in the short term but it becomes quite unrealistic for pricing long-dated contracts. Therefore, many studies have proposed the inclusion of a stochastic convenience yield as an additional variable in modeling the futures curves. We should also keep in mind that this spot-futures

relationship will collapse for non-storable commodities such as electricity, as the notion of convenience yield does not exist in these markets.

2.6 Rational Expectations Hypothesis under Risk-Neutral Measure

In the past, many studies by economists to test the validity of the rational expectations hypothesis in the futures market have been largely inconclusive. However, by following the methodology adopted by Geman (2005), we can show that under the assumption of no-arbitrage, the futures price is an unbiased predictor of the future spot price when the expectation is calculated under the risk-neutral measure Q. First of all, let us assume that the commodity spot price S_t can be described by the following stochastic differential equation:

$$\frac{dS_t}{S_t} = \mu \, dt + \sigma \, dW_t \tag{2.4}$$

where μ is the drift term of the process and W_t denotes a standard Brownian motion, which is a process with independent increments and such that $W_t - W_s$ follows a normal distribution with mean 0 and standard deviation $\sqrt{t-s}$. If we take the expectations on both sides of the equation, we obtain:

$$\mu = \frac{1}{dt} \, E_P\left[\frac{dS_t}{S_t} \mid \mathcal{F}_t\right]$$

which indicates that μ is the expected rate of return per unit of time where the only source of uncertainty is coming from the Wiener process W_t. Since the buyer of a futures contract is not entitled to the convenience yield and the Arbitrage Pricing Theory (Ross, 1976) states that the expected return of a risky asset can be modeled as a linear function

of various risk factors, we can further decompose μ into:

$$\mu = r + b - y$$

where r is the risk-free interest rate, b is the risk premium and y is the convenience yield. Next, we can introduce λ that represents the expected risk premium per unit of volatility given by $\lambda = \frac{b}{\sigma}$. By plugging λ into the equation above, we have:

$$\mu = r + \sigma\lambda - y.$$

Then, we substitute this expression into the stochastic differential equation (2.4) to obtain:

$$\frac{dS_t}{S_t} = (r - y)\,dt + \sigma(dW_t + \lambda\,dt).$$

From Girsanov's Theorem, there exists a special probability measure Q, which we call a risk-neutral measure, such that the process $\widehat{W}_t$ defined as:

$$d\widehat{W}_t = dW_t + \lambda\,dt$$

is a Q-Brownian motion. Therefore, under the risk-neutral probability measure Q, the price dynamics of a storable commodity take the form of:

$$\frac{dS_t}{S_t} = (r - y)\,dt + \sigma\,d\widehat{W}_t. \tag{2.5}$$

To justify that the futures price is an unbiased predictor of the future spot price at maturity and to show that the futures price is a martingale under the risk-neutral measure, we have to revisit the spot-futures relationship in equation (2.2):

$$F^T(t) = S_t e^{(r-y)(T-t)}.$$

We then differentiate both sides to obtain:

$$\frac{dF^T(t)}{F^T(t)} = \frac{dS_t}{S_t} - (r - y)\,dt. \tag{2.6}$$

By subtracting the dynamics of spot price (2.5) from the equation above, we get:

$$\frac{dF^T(t)}{F^T(t)} = \sigma\,d\widehat{W}_t \tag{2.7}$$

which represents the risk-neutral dynamics of the futures price.

Finally, we integrate equation (2.7) over the interval $[t, t_1]$ to provide:

$$F^T(t_1) = F^T(t)\,exp\left\{-\frac{\sigma^2}{2}(t_1 - t) + \sigma\widehat{W}(t_1 - t)\right\}.$$

Since $\widehat{W}(t_1 - t)$ follows a normal distribution, $F^T(t_1)$ is a log-normal variable with

parameters $m = \ln F^T(t) - \frac{\sigma^2}{2}(t_1 - t)$ and $\gamma = \sigma\sqrt{(t_1 - t)}$. The expected value of

a log-normal variable with parameters m and γ is known to be $e^{m+\frac{\gamma^2}{2}}$. Hence, the

expectation of $F^T(t_1)$ under the risk-neutral probability measure Q is given by

$F^T(t)e^{-\frac{\sigma^2(t_1-t)}{2}}e^{\frac{\sigma^2(t_1-t)}{2}}$ and this leads us to:

$$F^T(t) = E_Q[F^T(t_1)\,|\,\mathcal{F}_t] \quad \text{for any } t_1 > t. \tag{2.8}$$

From equation (2.8), we can see that under the risk-neutral measure Q, the futures

price process is a martingale and $F^T(t)$ should on the average remain constant. At

maturity time T, the futures price is denoted by $F^T(T)$ and under the no-arbitrage

assumption, this value should be equal to the spot price S_T. By substituting the spot

price at maturity into equation (2.8), we show that the futures price fulfills the condition for an unbiased predictor of the future spot price:

$$F^T(t) = E_Q[S_T \mid \mathcal{F}_t].$$

Hence, in the geometric Brownian motion setting, we have demonstrated that the rational expectations hypothesis holds for futures prices when the expectations are computed under the risk-neutral probability measure Q. In the context of interest rates, Bjork (1998) further showed that the forward interest rate is an unbiased estimator of the future spot rate when the expectation is computed under the forward neutral measure whereby the numeraire depends on the maturity of the payoff.

Chapter 3

Stochastic Modeling of Commodity Prices

The ability to formulate models to describe the dynamics of commodity prices is essential for traders and hedgers to properly price derivative contracts written on these assets. Many researchers have since proposed various stochastic models to represent the dynamics and seemingly random behaviour of commodity spot prices and futures curves. Rather than to provide accurate future price forecasts, these models are created to offer rigorous mathematical descriptions of commodity price dynamics by using properties observed in historical data. Such models should be chosen so that the stochastic process of commodity prices $S(t)$ results in a probability distribution that agrees with the empirical moments and other statistical features presented in the price data. The price trajectories simulated from these stochastic models should also be consistent with the dynamics of commodity prices that have been observed.

3.1 Returns Distribution of Commodity and Their Empirical Moments

Before we start discussing stochastic models that are commonly used in the representation of commodity price dynamics, we should first investigate the probability

distributions and empirical moments of commodity prices. Over long periods, stock prices generally exhibit upward trends as investors are rewarded for the long term growth in companies' earnings and dividend yields. In contrast, since supply and demand dictate the pricing in commodity markets, commodity prices typically show mean-reverting behaviour over a long period when demand and supply remain relatively stable. Figure 3.1 provides the best illustration of this scenario whereby the spot price of corn tends to mean-revert to its equilibrium level over the time span of 30 years with occasional spikes in price due to short term shocks to the supply and demand curves. In agreement with the theory of storage, we also observe that volatility increases when corn prices soar during periods of low inventories or adverse weather conditions. Next, we study the empirical
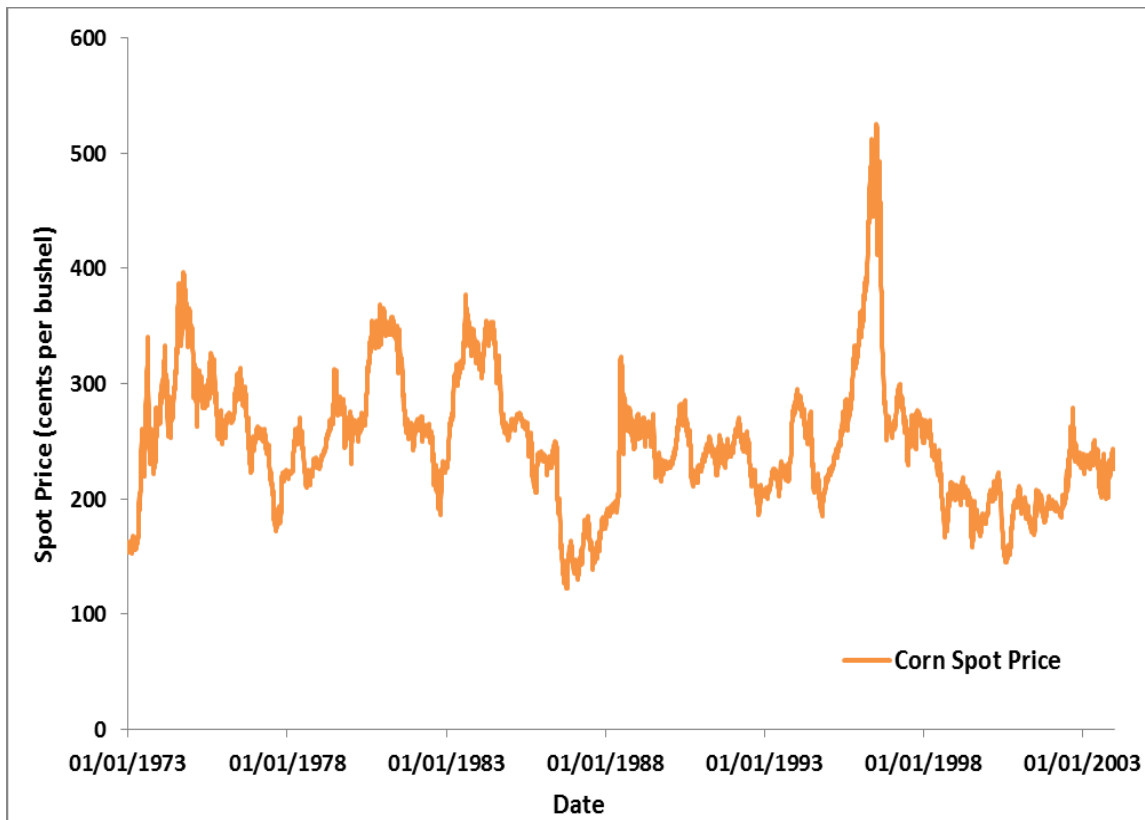
Figure 3.1 Spot price of corn over the period January 1973 to December 2003

moments of commodity returns to help us better understand the shapes of commodity returns distributions. Table 3.1 presents the first four moments calculated from daily logarithmic returns for several commodity spot prices, where the logarithmic return at time t is defined as $r_t = \ln(S_t/S_{t-1})$. The mean and standard deviation of daily log-returns are then being transformed into their annual equivalents (which are presented in the first two columns of Table 3.1) through the following formulas:

$$\mu_{annual} = e^{\mu_{daily} \times 260} - 1 \quad \text{and} \quad \sigma_{annual} = \sigma_{daily} \times \sqrt{260}.$$

Among all the commodities listed in Table 3.1, natural gas has the highest annualized volatility due to the fact that natural gas is expensive to store with limited storage facilities around the world. Moreover, price volatility increases during severe weather conditions when surging demand for natural gas coincides with the lack of pipeline capacity to deliver gas supply to meet the demand. On the other hand, metals (especially

Commodity	Mean	Standard Deviation	Skewness	Kurtosis
Light Sweet Crude Oil	0.1200	0.3980	-0.2496	7.5271
Natural Gas	0.1317	0.8940	1.2594	46.5225
Corn	-0.0558	0.2490	-0.1334	5.0005
Soybeans	-0.0207	0.2381	-0.5884	7.7576
Wheat	-0.0436	0.3014	0.1384	5.1103
Live Cattle	0.0352	0.2297	-0.4692	20.3232
Lean Hogs	0.0300	0.4837	0.5280	20.7038
Gold	0.0291	0.1333	0.5395	10.7159
Silver	0.0570	0.2162	-0.3680	7.6401
Copper	0.0532	0.2413	-0.6068	9.7800
Cocoa	0.0167	0.2871	0.3940	9.8483
Sugar No. 11	0.0249	0.3280	-0.4141	9.3942
Cotton	-0.0405	0.2828	0.0057	5.6872

Table 3.1 First four moments of commodity log-returns over the period January 1996 to December 2005

gold and silver) are less volatile than other commodities, since they are easy to stock and inventories are available to absorb any shocks in demand. We also observe that for all commodities in Table 3.1, their kurtoses are greater than 3, which indicate that their return distributions have heavier tails than the normal distribution and the occurrence of extreme or "black swan" events are relatively more frequent. It is important that these high values of kurtosis are properly represented when we are designing methodology to compute the Value-at-Risk or other risk measures for commodity investments, so that the true risk of these investments is not understated.

3.2 Geometric Brownian Motion

In 1965, Paul Samuelson proposed the use of geometric Brownian motion to model the dynamics of stock price. Currently, geometric Brownian motion is still widely used among practitioners to describe the behaviour of stock prices and it forms the basis for Black-Scholes option pricing model. The stock price S_t is considered to follow a geometric Brownian motion if its stochastic process satisfies the following equation:

$$\frac{dS_t}{S_t} = \mu \, dt + \sigma \, dW_t$$

where μ and σ are respectively the constant drift and constant volatility terms and W_t is a Wiener process. From the equation above, we note that under the assumption of geometric Brownian motion, the expected stock price grows over time by a rate given by the drift term μ. Since commodity prices exhibit mean-reverting behaviour and do not generally display trends over long periods, geometric Brownian motion might not be an appropriate model for commodity prices. Therefore, in Section 3.3, we will introduce a

mean-reversion model that aims at capturing and describing the dynamics of commodity prices. Moreover, the assumption of constant volatility is not in line with the fact that volatility of commodity prices varies over time as a consequence of changing storage level. Later in this chapter, we discuss models which allow for changing volatility through the introduction of stochastic volatility or by adding a jump component to the model. Lastly, geometric Brownian motion also implies that log-returns for stocks are normally distributed since the quantity $(\mu \, dt + \sigma \, dW_t)$ is a normal variable. From Section 3.1, we observe that commodity returns show obvious deviations from normality and therefore we should carefully examine the robustness of using geometric Brownian motion to model commodity prices.

3.3 Mean-Reverting Model for Commodities

In this section, we will look at several mean-reverting models which are commonly used to describe the random evolution of commodity prices. In 1977, Vasicek suggested that short-term interest rates, which typically fluctuate in a narrow range, can be modeled with an Ornstein-Uhlenbeck process which satisfies the following stochastic differential equation:

$$dr_t = a \, (b - r_t) \, dt + \sigma \, dW_t.$$

In this equation, b represents the mean level where the short rate will evolve around in the long run and a is the rate of reversion that characterizes the speed at which future trajectories will revert back to b. However, we should note that the model allows the short rate r_t to take negative values, which is an undesirable feature for modeling

commodity prices. To remedy this problem, Schwartz (1997) considers the following model for commodity spot prices:

$$\frac{dS_t}{S_t} = k(\theta - \ln S_t) \, dt + \sigma \, dW_t \tag{3.1}$$

where the rate of return for commodity $\frac{dS_t}{S_t}$ is a normal variable, which demonstrates the fact that negative values are admissible for commodity returns. If we introduce $Z_t = \ln S_t$ and apply the Ito's lemma, we have:

$$dZ_t = k\left(\theta - \frac{\sigma^2}{2k} - Z_t\right) dt + \sigma \, dW_t \tag{3.2}$$

meaning that the log price Z_t can be described in the form of an Ornstein-Uhlenbeck stochastic process. We further define variable $X_t = e^{kt}Z_t$ and again, by using Ito's lemma, we get:

$$dX_t = e^{kt} \, dZ_t + k \, e^{kt} \, Z_t \, dt.$$

By substituting equation (3.2) into the equation above, we obtain:

$$dX_t = k\left(\theta - \frac{\sigma^2}{2k}\right) e^{kt} \, dt + \sigma \, e^{kt} \, dW_t. \tag{3.3}$$

Next, we integrate equation (3.3) over the interval $[t, T]$ to get:

$$X_T = X_t + \left(\theta - \frac{\sigma^2}{2k}\right)(e^{kT} - e^{kt}) + \sigma \int_t^T e^{ks} \, dW_s. \tag{3.4}$$

Since $X_t = e^{kt}Z_t$, equation (3.4) becomes:

$$Z_T = e^{-k(T-t)} Z_t + \left(\theta - \frac{\sigma^2}{2k}\right)\left(1 - e^{-k(T-t)}\right) + \sigma \, e^{-kT} \int_t^T e^{ks} \, dW_s.$$

We notice from the equation above that process Z_T is normally distributed with mean $e^{-k(T-t)} Z_t + \left(\theta - \frac{\sigma^2}{2k}\right)\left(1 - e^{-k(T-t)}\right)$ and variance:

$$Var(Z_T) = Var\left(\sigma e^{-kT} \int_t^T e^{ks} \, dW_s\right) = \sigma^2 e^{-2kT} E\left[\left(\int_t^T e^{ks} \, dW_s\right)^2\right].$$

With Ito's Isometry, we have:

$$Var(Z_T) = \sigma^2 e^{-2kT} E\left[\left(\int_t^T e^{ks} \, dW_s\right)^2\right] = \sigma^2 e^{-2kT} \int_t^T e^{2ks} \, ds$$

$$= \frac{\sigma^2}{2k}\left(1 - e^{-2k(T-t)}\right).$$

Since $S_T = e^{Z_T}$, process S_T will follow a log-normal distribution with parameters $\mu = e^{-k(T-t)} \ln S_t + \left(\theta - \frac{\sigma^2}{2k}\right)\left(1 - e^{-k(T-t)}\right)$ and $\gamma^2 = \frac{\sigma^2}{2k}\left(1 - e^{-2k(T-t)}\right)$. Under the assumption that the rational expectations hypothesis holds, we have shown in the previous chapter that futures price $F^T(t)$ can be computed by equating $F^T(t) = E[S_T \mid \mathcal{F}_t]$. Given that the expected value of log-normal variable S_T is known to be $e^{\mu + \frac{\gamma^2}{2}}$, we have:

$$F^T(t) = \exp\left\{e^{-k(T-t)} \ln S_t + \left(\theta - \frac{\sigma^2}{2k}\right)\left(1 - e^{-k(T-t)}\right) + \frac{\sigma^2}{4k}\left(1 - e^{-2k(T-t)}\right)\right\}.$$

Therefore, the process (3.1) provides a simple one-factor model that is capable of describing the mean-reverting feature of commodity prices and yields a closed-form solution for futures prices.

3.4 Stochastic Convenience Yield Model

In Chapter 2, we argued that convenience yield plays an important role in explaining the term structure of commodity prices. Gabillon (1991) remarked that dissimilar shapes of contango and backwardation manifested over time in commodity markets contradict the assumption of a constant convenience yield. Hence, it is reasonable to introduce convenience yield as an additional state variable to improve the quality of modeling. Gibson and Schwartz (1990) developed a two factor model by including the instantaneous net convenience yield δ_t as the second state variable to model oil contingent claims. The joint diffusion process of Gibson and Schwartz model is specified in the form:

$$\frac{dS_t}{S_t} = (\mu - \delta_t)\, dt + \sigma_1\, dW_t^1$$

$$d\delta_t = \kappa\, (\alpha - \delta_t)\, dt + \sigma_2\, dW_t^2$$

where the two Brownian risk factors are correlated such that $dW_t^1\, dW_t^2 = \rho\, dt$. According to the model, the process of commodity price S_t is a geometric Brownian motion where the growth rate is adjusted by a net convenience yield δ_t. Motivated by their study on the time series properties of forward convenience yields of crude oil, the stochastic convenience yield δ_t follows an Ornstein-Uhlenbeck process to assert its mean-reverting pattern. Since convenience yield is positively correlated to the spot price (that is $\rho > 0$), a decline in spot price S_t will result in a decrease in the convenience yield δ_t. A lower convenience yield will cause the spot price process to have a larger drift rate and hence will drive up the spot price for next period. Therefore, the spot price process

exhibits some kind of mean-reversion behaviour through the influence of convenience yield from both the correlation coefficient and the drift term of the process. Under the risk-neutral measure Q, the risk-adjusted stochastic processes can be re-written as follows:

$$\frac{dS_t}{S_t} = (r - \delta_t)\,dt + \sigma_1\,d\overline{W}_t^1$$

$$d\delta_t = [\kappa\,(\alpha - \delta_t) - \lambda]\,dt + \sigma_2\,d\overline{W}_t^2$$

$$d\overline{W}_t^1\,d\overline{W}_t^2 = \rho\,dt$$

with λ representing the market price of convenience yield risk. Since the risk associated with convenience yield cannot be hedged with any tradable products, the risk neutral convenience yield process will contain a risk premium for bearing the risk. By using Ito's lemma and with the absence of any arbitrage opportunity, it can be shown that futures price $F(S_t, \delta_t, t, T)$ must satisfy the following partial differential equation (see Gibson and Schwartz (1990) for a detailed derivation):

$$\frac{1}{2}\sigma_1^2 S_t^2 F_{ss} + \sigma_1\sigma_2\rho S_t F_{s\delta} + \frac{1}{2}\sigma_2^2 F_{\delta\delta} + (r - \delta_t)S_t F_s + (\kappa(\alpha - \delta_t) - \lambda)F_\delta - F_t = 0$$

subject to the terminal boundary condition $F(S_T, \delta_T, T, T) = S_T$. Jamshidian and Fein (1990) and Bjerksund (1991) derived an analytical solution to this equation, which can be expressed as:

$$F(S_t, \delta_t, t, T) = S_t\,exp\left[-\delta_t\frac{1 - e^{-\kappa(T-t)}}{\kappa} + A(T - t)\right]$$

where

$$A(T - t) = \left(r - \hat{\alpha} + \frac{1}{2}\frac{\sigma_2^2}{\kappa^2} - \frac{\sigma_1\sigma_2\rho}{\kappa}\right)(T - t) + \frac{1}{4}\sigma_2^2\frac{1 - e^{-2\kappa(T-t)}}{\kappa^3}$$

$$+ \left(\hat{\alpha}\kappa + \sigma_1\sigma_2\rho - \frac{\sigma_2^2}{\kappa}\right)\frac{1 - e^{-\kappa(T-t)}}{\kappa^2}$$

and $\hat{\alpha} = \alpha - \frac{\lambda}{\kappa}$. Hence, Gibson and Schwartz have provided a tractable model to value commodity futures contracts, which includes convenience yield as the second stochastic factor.

3.5 Stochastic Volatility Models and Jump Diffusion Process

The stochastic models that we have discussed in previous sections are based on the assumption that volatility stays constant over time. However, the volatility of commodity prices tends to increase when the price level is high. On the other hand, commodity prices are less volatile when abundant inventory is available to buffer any shocks in the demand-supply balance. Therefore, it will be desirable for us to relax the assumption of constant volatility by introducing stochastic volatility model or by adding a jump component to the existing models.

By extending the Heston (1993) model, Eydeland and Geman (1998) proposed a stochastic volatility model that maintains the mean-reversion behaviour in commodity spot prices. The joint stochastic process of the two state variables is described as follows:

$$\frac{dS_t}{S_t} = \kappa(\theta - lnS_t)\,dt + \sqrt{v_t}\,dW_t^1$$

$$dv_t = b(\alpha - v_t)\,dt + \xi\,\sqrt{v_t}\,dW_t^2$$

$$dW_t^1\,dW_t^2 = \rho\,dt$$

37

where ξ is the volatility of volatility which determines the variance of v_t. Since commodity price is more volatile when the price level increases, the correlation coefficient ρ which relates the two Brownian motions is typically positive. In this model, the instantaneous variance v_t is characterized by a Cox-Ingersoll-Ross (CIR) model to represent the mean reversion of the price variance towards its long run mean level α and to ensure the process v_t remains strictly positive if the parameters obey the condition of $2b\alpha \geq \xi^2$. As standard deviation of the instantaneous variance process is defined by $Std(dv_t) = \xi\sqrt{v_t}$, when price variance v_t approaches zero, the effect of random shock component becomes minimal and the evolution of v_t is mainly dominated by the drift term that pushes the price variance away from zero towards the mean level to prevent the possibility of negative volatility. In order to further improve the quality of this model, Richter and Sorensen (2002) proposed a model that incorporates stochastic convenience yield and stochastic volatility. Without the stochastic volatility component, the model suggested by Richter and Sorensen corresponds to the Gibson and Schwartz model we discussed in Section 3.4.

For certain commodity markets which exhibit higher volatility in their price movements, particularly electricity and natural gas, it is quite common for us to observe sharp and unanticipated spikes in the price data. The sudden jumps in commodity prices are normally the result of political unrests or severe weather conditions which cause disruptions in the supply or escalations in consumer demand. Figure 3.2 depicts the evolution of the Henry Hub natural gas spot price for period in between May 1995 and May 2006. We notice that cash price of natural gas has occasional spikes over this period,

38

generally due to sustained cold weather in the winter which causes a hike in heating demand.
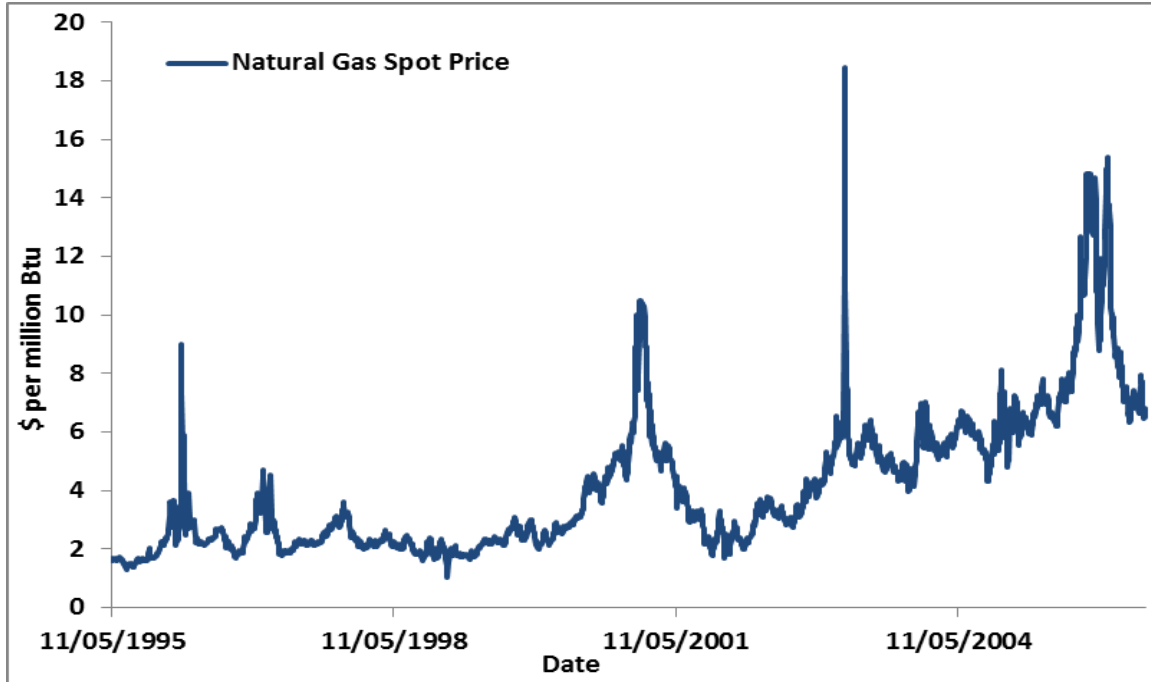
Figure 3.2 Daily Henry Hub Natural Gas spot price from May 1995 to May 2006

In order to accommodate this phenomenon in commodity prices, it is appropriate to include a jump component to the diffusion process (3.1) we discussed above. In an influential paper published in 1976, Merton first introduced a jump diffusion model for stock returns. To better represent the heavy tails in returns distribution, the spot price dynamics can be described with the following stochastic differential equation:

$$\frac{dS_t}{S_t} = \mu \, dt + \sigma \, dW_t + U_t \, dN_t$$

where N_t accounts for the frequency of jumps. Here, N_t follows a Poisson process with parameter λ which is the expected number of jumps that occur per year. Furthermore, the

size or magnitude of jumps is denoted by U_t which is a normally distributed random variable that takes positive and negative values. We can further extend this model to include mean-reversion behaviour by having the following stochastic process:

$$\frac{dS_t}{S_t} = k(\theta - \ln S_t)\, dt + \sigma\, dW_t + U_t\, dN_t$$

where the model is a mixture of a jump component and a diffusion process governed by Schwartz's (1997) one-factor model. However, since the process has to mean-revert quickly after a huge jump, the mean-reversion rate k necessary to bring the spike back to its normal levels would be unrealistically large. This in turn will cause the diffusion components for standard daily moves to revert to the mean level instantaneously and the paths would appear deterministic.

Chapter 4

Stochastic Long-Run Mean Models

In the previous chapter, we have presented models that incorporate the empirical fact that in the long run commodity prices will mean-revert to a constant price level. In this chapter, we are going to provide an additional degree of randomness to this long-run mean level by allowing it to follow a stochastic process. This in turn will offer a more flexible model and, as a result, help better describe the term structure of commodity futures prices with maturities extending into months or years. Pilipovic (1997) first adapted the idea of a changing mean level by introducing a two-factor stochastic model that satisfies the following differential equations:

$$dS_t = \beta(\theta_t - S_t)\,dt + \sigma_S\,S_t\,dW_t^1$$

$$\frac{d\theta_t}{\theta_t} = \alpha\,dt + \sigma_\theta\,dW_t^2$$

$$dW_t^1\,dW_t^2 = \rho\,dt.$$

Here, the spot price process will mean-revert to a stochastic long-run mean denoted by θ_t. Meanwhile, the stochastic mean level θ_t follows a geometric Brownian motion with a drift term α. Therefore, according to the model, long-run mean will grow over time at a rate of α. However, a Brownian motion with a positive drift term may, with a positive probability, never return to the origin. Hence, one possible limitation to this model is that the long-run mean might grow without bound and causes the spot price process to be non-stationary. In order to get around this problem, Hikspoors and Jaimungal (2007) proposed a two-factor model such that the stochastic mean level also mean-reverts to a second long-run mean to maintain the stationary behaviour of the underlying spot price process. To translate the seasonal feature in commodity prices, the spot price S_t is defined as:

$$S_t = exp(g_t + X_t) \tag{4.1}$$

where g_t represents the seasonality term, which is normally a function expressed as a sine or cosine with annual periodicity. In addition, Hikspoors and Jaimungal complete the specification of the two-factor model by assuming X_t to satisfy the following joint stochastic process:

$$dX_t = \beta(Y_t - X_t)\, dt + \sigma_X\, dW_t \tag{4.2}$$

$$dY_t = \alpha(\phi - Y_t)\, dt + \sigma_Y\, dZ_t \tag{4.3}$$

where the two Brownian motions, W_t and Z_t are correlated such that $dW_t dZ_t = \rho\, dt$. In this model, X_t mean-reverts to the stochastic mean level Y_t with the rate denoted by β while α dictates the mean-reversion speed of Y_t towards the constant long-run mean ϕ.

To relax the assumption of constant volatility, Hikspoors and Jaimungal (2008) further extend this model to allow for a stochastic volatility component in the spot price process. The joint stochastic process for this model can be written in the form:

$$dX_t = \beta(Y_t - X_t)\, dt + \sqrt{v_t}\, dW_t^1$$

$$dY_t = \alpha(\phi - Y_t)\, dt + \sigma_Y\, dW_t^2$$

$$dv_t = b(m - v_t)\, dt + \xi\, \sqrt{v_t}\, dW_t^3$$

with the correlation structure,

$dW_t^1 dW_t^2 = \rho_1 dt$, $dW_t^1 dW_t^3 = \rho_2 dt$, and $dW_t^2 dW_t^3 = 0$.

This structure allows the main driving factor X_t to be correlated to its own stochastic volatility component v_t and to the long-run mean-reverting level Y_t. Since the volatility component v_t describes the short-term fluctuations in commodity prices, it is also reasonable to assume that v_t is not related to the long-run mean level Y_t that changes slowly over time. The volatility of X_t is again being characterized by a mean-reverting stochastic process.

4.1 Hikspoors and Jaimungal Two-Factor Mean-Reverting Model

For the rest of the thesis, we will focus on studying the two-factor mean-reverting model proposed by Hikspoors and Jaimungal, which will be referred to as the "HJ Model" from here onwards. In their paper, Hikspoors and Jaimungal provide a framework for modeling spot prices of energy commodities and demonstrate that the calibration procedure produces stable estimation of the model parameters for the NYMEX Light Sweet Crude

Oil spot and futures data. Moreover, within this modeling framework, they are able to derive closed form pricing equations for futures contract and various spread options. Having successfully estimated both the risk-neutral and real-world parameters, the authors can subsequently extract the implied market prices of risk for these commodities. To examine the versatility of this framework, in this thesis we will focus on testing the robustness of the calibration process by applying the methodology to simulated data. The capability of this calibration process to produce stable estimates of the model parameter from various initial guesses will be assessed. We also explore the possible presence of model uncertainty which leads to the miscalculation of market prices of risk as a consequence of multiple solutions given by the calibration process.

In the HJ Model, the spot price, S_t, is an exponential function of the seasonal component, g_t, and the main driving factor, X_t, as we have seen in equation (4.1). Since seasonality represents an important feature observed in certain commodity prices, the authors have further specified g_t as a function of cosine and sine:

$$g_t = A_0 t + \sum_{k=1}^{n}(A_k \sin(2\pi kt) + B_k \cos(2\pi kt)) \tag{4.4}$$

where n is typically chosen to have value of 1 or 2 to assure stability in the calibration process. The two-factor mean-reverting model which drives the spot price process is then being described by equations (4.2) and (4.3). To find a solution to these equations, we will first solve the stochastic differential equation that involves the long-run mean Y_t. Since Y_t follows the standard Ornstein-Uhlenbeck process, by applying Ito's lemma to solve equation (4.3), we get:

$$Y_t = \phi + (Y_s - \phi)\, e^{-\alpha(t-s)} + \sigma_Y \int_s^t e^{-\alpha(t-u)}\, dZ_u. \tag{4.5}$$

Next, we substitute this result into equation (4.2) and solve for X_t while taking into account the correlation between X_t and Y_t to obtain:

$$X_t = G_{s,t} + e^{-\beta(t-s)} X_s + M_{s,t} Y_s + \sigma_X \int_s^t e^{-\beta(t-u)} \, dW_u + \sigma_Y \int_s^t M_{u,t} \, dZ_u \qquad (4.6)$$

where $M_{s,t}$ and $G_{s,t}$ are two deterministic functions defined as:

$$M_{s,t} = \gamma(e^{-\beta(t-s)} - e^{-\alpha(t-s)}) \qquad (4.7)$$

$$G_{s,t} = \phi(1 - e^{-\beta(t-s)}) - \phi M_{s,t} \qquad (4.8)$$

and $\gamma = \dfrac{\beta}{\alpha - \beta}$. Having the solutions (4.5)-(4.6) for the two-factor model, we can proceed with the valuation of commodity futures contracts in two distinct scenarios – real-world and risk-neutral.

4.1.1 An Actuarial Approach for Pricing Commodity Futures

For the purpose of pricing a derivative contract, it is common that one will adopt a risk-neutral approach to this problem. Under the assumption that markets are arbitrage-free, there exists at least one risk-neutral measure such that all traded assets must have the same expected rate of return – the risk-free interest rate. The advantage of using this approach comes from the fact that once the risk-neutral probabilities are discovered, every asset in the market can be priced by taking the expectation of its future payoff without adjustment for any individual's risk preference. However, Hikspoors and Jaimungal have suggested that it may be inappropriate to adopt a risk-neutral framework for pricing commodity derivatives based on the argument that commodity spot markets are fairly illiquid. Moreover, Hull (2005) justifies the use of an Actuarial approach for

pricing derivatives by assuming the risks associated with commodity prices are non-diversifiable. Therefore, following Hikspoors and Jaimungal, we will present the derivation of commodity futures prices under an Actuarial valuation framework where expectations are computed to reflect real-world beliefs of possible future outcomes.

In their paper, Hikspoors and Jaimungal have defined the pseudo-forward price process, $H_{t,T}$, as the following:

$$H_{t,T} = E_P[S_T \mid \mathcal{F}_t] \tag{4.9}$$

where the conditional expectation is computed under a real-world probability measure, P, with $\mathcal{F}_t$ signifying the information available in the market at time t. From what we have learned in Chapter 2, if the conditional expectation is computed under a risk-neutral measure Q, equation (4.9) represents the rational expectations hypothesis which implies that the futures price is an unbiased predictor of the future spot price at maturity.

By assuming that the rational expectations hypothesis holds in a real-world setting, equation (4.9) offers a method to derive a closed-form solution for commodity futures prices under an Actuarial valuation framework. By substituting the definition of spot price process from equation (4.1) into equation (4.9), we obtain:

$$H_{t,T} = E_P[exp(g_T + X_T) \mid \mathcal{F}_t].$$

Using equation (4.6) for X_T, we can further expand the equation above and compute the expectation to get:

$$H_{t,T} = E_P \left[\exp\left(g_T + G_{t,T} + e^{-\beta(T-t)}X_t + M_{t,T}Y_t + \sigma_X \int_t^T e^{-\beta(T-u)} \, dW_u \right. \right.$$

$$\left. \left. + \sigma_Y \int_t^T M_{u,T} \, dZ_u \right) \mid \mathcal{F}_t \right]$$

$$= \exp\left(g_T + G_{t,T} + R_{t,T} + e^{-\beta(T-t)}X_t + M_{t,T}Y_t \right) \tag{4.10}$$

where the expressions for $M_{t,T}$ and $G_{t,T}$ are supplied in Equations (4.7) and (4.8) respectively while $R_{t,T}$ is defined as follows:

$$R_{t,T} = \frac{h(t,T;2\beta)}{2}[(\sigma_X)^2 + (\gamma\sigma_Y)^2 + 2\rho\gamma\sigma_X\sigma_Y] - h(t,T;\alpha+\beta)[(\gamma\sigma_Y)^2 + \rho\gamma\sigma_X\sigma_Y]$$

$$+ \frac{h(t,T;2\alpha)}{2}(\gamma\sigma_Y)^2$$

with

$$h(t,T;a) = (1 - e^{-a(T-t)})/a.$$

Hence, with equation (4.10), we have a closed-form solution for the commodity futures price derived under the real-world probability measure P.

4.1.2 Risk-Neutral Pricing of Commodity Futures Contract

To preserve the fundamental assumption of no-arbitrage, the risk-neutral approach has been heavily used in the pricing of derivative products. In a complete market setting, there exists a unique risk-neutral measure that results in a unique arbitrage-free price for any derivative contract. Given the illiquidity in commodity spot trading and the fact that certain risks associated with commodity prices are non-diversifiable, there may exist a multitude of equivalent risk-neutral measures within such incomplete markets. It is then

through the trading of these derivative contracts that the market as a whole will determine which measure will prevail at any given point in time. In order to solve for futures prices, we proceed to introduce a class of equivalent risk-neutral measures that maintains the real-world structure of price dynamics.

To obtain a set of risk-neutral measures, Q, Hikspoors and Jaimungal begin with a change of measure by introducing the Radon-Nikodym derivative, ζ_t, such that:

$$\zeta_t = \left(\frac{dQ}{dP}\right)_t = \mathcal{E}\left(\int_0^t \{\lambda_u\, dW_u + \psi_u dZ_u\}\right)$$

where $\mathcal{E}(A_t)$ represents the Dolean-Dade's exponential of A_t. By decomposing the correlated processes into uncorrelated processes and applying Girsanov's Theorem, Hikspoors and Jaimungal go on to introduce the following Q-Wiener processes:

$$\overline{W}_t = W_t - \int_0^t \{\lambda_u + \rho\psi_u\}\, du \tag{4.11}$$

$$\overline{Z}_t = Z_t - \int_0^t \{\rho\lambda_u + \psi_u\}\, du \tag{4.12}$$

where the two Q-Wiener processes are correlated such that $d\overline{W}_t d\overline{Z}_t = \rho dt$.

Due to the incompleteness of commodity markets, there exists a huge number of possible prices for a derivative contract, each corresponding to different risk neutral measures Q. Therefore, Hikspoors and Jaimungal have suggested that by applying some constraints on the market prices of risk, the risk-neutral dynamics of X_t and Y_t will be of the same form as they were under the real-world probability measure. In particular, X_t and Y_t under the risk-neutral measure will be described in the form of:

$$dX_t = \bar{\beta}(Y_t - X_t)\,dt + \sigma_x\,d\overline{W}_t \qquad (4.13)$$

$$dY_t = \bar{\alpha}(\bar{\phi} - Y_t)\,dt + \sigma_Y\,d\overline{Z}_t. \qquad (4.14)$$

However, we note that even though the risk neutral and the real-world dynamics are of the same form, the parameters $\bar{\alpha}$, $\bar{\beta}$ and $\bar{\phi}$ which drive the risk-neutral dynamics may be significantly different from those under the real-world measure in Equations (4.2)-(4.3). This feature enables us to simultaneously calibrate the model parameters for the risk-neutral and the real-world dynamics. Going back to the suggestion by Hikspoors and Jaimungal, they have shown in their paper that, if the market prices of risk are chosen such that:

$$\lambda_t = \lambda + \lambda_X X_t + \lambda_Y Y_t \qquad (4.15)$$

$$\psi_t = \psi + \psi_X X_t + \psi_Y Y_t \qquad (4.16)$$

subject to the following constraints,

$$\psi_X = -\rho\lambda_X \qquad (4.17)$$

$$\lambda + \rho\psi = 0 \qquad (4.18)$$

$$\lambda_X + \rho\psi_X = -(\lambda_Y + \rho\psi_Y) \qquad (4.19)$$

$$\bar{\alpha} = \alpha - \sigma_Y(\rho\lambda_Y + \psi_Y) \qquad (4.20)$$

$$\bar{\alpha}\bar{\phi} = \left(\alpha\phi + \sigma_Y(\rho\lambda + \psi)\right) \qquad (4.21)$$

$$\bar{\beta} = \beta + \sigma_X(\lambda_Y + \rho\psi_Y) \qquad (4.22)$$

then the risk-neutral dynamics will remain in the same class as those in the real-world settings.

Once we have the risk-neutral dynamics of the diffusion processes to be in the form of equations (4.13)-(4.14), it will be straightforward for us to derive a closed-form solution for commodity futures price under the risk-neutral measure Q. Since the rational expectations hypothesis holds within the risk-neutral framework, the commodity futures price is defined as:

$$F_{t,T} = E_Q[S_T \mid \mathcal{F}_t]$$

which is analogous to the pseudo-forward price we defined in equation (4.9). Hence, by extracting from equation (4.10), the futures price associated with a risk-neutral measure is given by:

$$F_{t,T} = \exp\left(g_T + \bar{G}_{t,T} + \bar{R}_{t,T} + e^{-\bar{\beta}(T-t)}X_t + \bar{M}_{t,T}Y_t\right) \tag{4.23}$$

where all the P-parameters are changed to Q-parameters. Therefore, with equation (4.23), we have obtained an expression for commodity futures price curves in terms of some elementary functions.

Chapter 5

Model Calibration and Its Robustness

After a detailed review of the HJ Model, in this chapter we will discuss the subjects of parameter estimation and the robustness of the calibration procedure. First, we present a calibration methodology proposed by Hikspoors and Jaimungal to estimate the parameters for this two-factor diffusion model. Using this method, both the risk-neutral and real-world parameters can be obtained through the calibration of the HJ Model to the spot and futures prices. Once the risk-neutral and real-world parameters are estimated, the authors further proposed an approach to extract the implied market prices of risk. Hence, in Section 5.4, we will investigate the robustness of this process by applying the methodology to simulated data to examine its ability to produce stable estimates of the true parameter values which are used in generating these data. In addition, we study the sensitivity of the calibration results with regard to different selections of initial guesses for the model parameters. Finally, we discuss how the calculation of market prices of risk might be exposed to model uncertainty as a result of multiple solutions produced by the calibration procedure.

5.1 Calibration Methodology

From previous chapter, we recall that the log futures price under the risk-neutral measures Q is given by:

$$\log F_{t,T} = g_T + \bar{G}_{t,T} + \bar{R}_{t,T} + e^{-\bar{\beta}(T-t)}X_t + \bar{M}_{t,T}Y_t \tag{5.1}$$

$$= g_T + \bar{G}_{t,T} + \bar{R}_{t,T} + e^{-\bar{\beta}(T-t)}(\log S_t - g_t) + \bar{M}_{t,T}Y_t \tag{5.2}$$

where S_t is the spot price of the commodity and g_t represents the seasonality component. To simplify the notation, the function $\bar{U}_{t,T}$ is being introduced such that:

$$\log F_{t,T} = \bar{U}_{t,T} + \bar{M}_{t,T}Y_t. \tag{5.3}$$

The long-run mean level Y_t in equation (5.3) cannot be directly observed from the market price data. Hence, we have to express this latent factor as a function of the remaining model parameters and obtain a least-squares estimate of Y_t that best fits the observed futures curves. For each given time t_p, we can obtain the long-run mean level in terms of risk-neutral model parameters $\bar{\Theta}$ such that it minimizes the following sum of squared differences between the observed log futures price and the calculated value provided by equation (5.3):

$$Sum(t_p, \bar{\Theta}) = \sum_{q=1}^{n_p} [\bar{U}_{t_p, T_q^p} + \bar{M}_{t_p, T_q^p} Y_{t_p} - \log F^*_{t_p, T_q^p}]^2 \tag{5.4}$$

where $F^*_{t_p, T_q^p}$ refers to the observed futures price at time t_p with contract maturity time T_q^p. Therefore, the optimal value for long-run mean level, $Y_{t_p}^{\#}(\bar{\Theta})$, can be solved to be:

$$Y_{t_p}^{\#}(\overline{\Theta}) = \frac{\sum_{q=1}^{np} [\overline{M}_{t_p,T_q^p}\left(logF^*_{t_p,T_q^p} - \overline{U}_{t_p,T_q^p}\right)]}{\sum_{q=1}^{np} [\overline{M}_{t_p,T_q^p}]^2}. \tag{5.5}$$

To estimate the risk-neutral model parameters $(\bar{\beta}, \bar{\alpha}, \bar{\phi}, \sigma_X, \sigma_Y, \rho)$, we first substitute the

optimal $Y_{t_p}^{\#}(\overline{\Theta})$ into equation (5.4) and sum it over the range of times $\{t_p\}$. Subsequently,

we look for the optimal risk-neutral parameters $\overline{\Theta}^*$ by performing an optimization

procedure described by the following function:

$$\overline{\Theta}^* = ArgMin_{\overline{\Theta} \in \overline{\Omega}} \sum_{p=1}^{m} \sum_{q=1}^{n_m} [\overline{U}_{t_p,T_q^p} + \overline{M}_{t_p,T_q^p} Y_{t_p}^{\#} - logF^*_{t_p,T_q^p}]^2. \tag{5.6}$$

Hence, by using this methodology, we are able to obtain a set of optimal risk-neutral

model parameters $\overline{\Theta}^*$ which provides a best fit of the model to the futures prices.

Next, we proceed to estimate the model parameters $(\beta, \alpha, \phi, \sigma_X, \sigma_Y, \rho)$ under the

real-world measure P. From Girsanov's Theorem, we know that the volatility structure

will remain unaltered after a change of measure from the real-world to the risk-neutral.

As a result, σ_X, σ_Y and ρ under the P-measure can be easily obtained from the calibration

results given by equation (5.6). To estimate the remaining set of P-parameters, we first

assume that a one-factor mean-reverting model for X_t (equation (4.2)) will act as a proxy

to our two-factor model. By discretizing the time steps of equation (4.2) and rearranging

the terms, we get:

$$X_t - X_{t-1} = \beta Y_{t-1}\Delta t - \beta\Delta t X_{t-1} + \sigma_X \Delta W_t. \tag{5.7}$$

We further assume that the stochastic long-run mean level Y_t in the equation above

becomes our constant one-factor mean-reversion level ϕ. Therefore, we can use equation

(5.7) to perform a linear regression on the spot price data to find least-squares estimates of β and ϕ. We subsequently use the estimated hidden mean process $Y_t^\#$ given by equation (5.5) as a data set to perform a similar linear regression for the discretized model of equation (4.3) in order to obtain the estimated value of α.

Once we have obtained the risk-neutral and the real-world model parameters, we can further extract the implied market prices of risk for the given commodity market. The evolutions of the implied market prices of risk λ_t and ψ_t described as follows:

$$\lambda_t = \lambda + \lambda_X X_t + \lambda_Y Y_t \tag{5.8}$$

$$\psi_t = \psi + \psi_X X_t + \psi_Y Y_t \tag{5.9}$$

can be easily solved subject to the constraints listed in equations (4.17)-(4.22).

5.2 Light Sweet Crude Oil Futures Contract

For the purpose of testing the robustness of the calibration procedure, we apply the methodology to simulated data obtained from a model fitted to the price dynamics of Light Sweet Crude Oil (WTI) futures contracts. For this reason, it will be useful for us to provide a brief description of the WTI futures contract. The WTI futures contracts trade on the New York Mercantile Exchange (NYMEX) and they represent the world's most actively traded futures contract on a physical commodity. To offer liquidity and price transparency, crude oil futures have a well-developed term structure with maturities spanning over nine years. Monthly contracts are listed for the current year and the next five years while only the June and December contract months are traded from the sixth year onward. During the delivery month, a single futures contract calls for the delivery of

1000 barrels of crude oil at Cushing, Oklahoma. Meanwhile, the last trading day of a futures contract is the third business day prior to the 25th calendar day of the month preceding the delivery month. In our calibration process, we therefore calculate the time-to-maturity for different futures contract months by choosing the last day of trading as the expiration date of a contract.

5.3 Simulation of the HJ Model

For the purpose of our investigation, we simulate 30 distinct sample paths of crude oil prices on the assumption that the spot price dynamics follow the HJ Model. Each sample path is simulated with 1500 observations by using the following risk-neutral parameter values for HJ Model:

$\bar{\alpha}$	$\bar{\beta}$	$\bar{\phi}$	σ_X	σ_Y	ρ
0.15	0.31	3.27	0.33	0.63	-0.96

Table 5.1 Parameter values used in simulating crude oil prices

The parameter values in Table 5.1 are chosen for our simulation process since these values represent the calibration result obtained by Hikspoors and Jaimungal after applying the HJ Model to the NYMEX WTI futures data for the period of 01/10/2003 to 25/07/2006.

To simulate a path following the HJ Model, we first apply the Euler method to discretize the joint stochastic process (4.2)-(4.3) with a time step equal to one trading day:

$$X_t = X_{t-1} + \beta(Y_{t-1} - X_{t-1})\Delta t + \sigma_X \Delta W_t \tag{5.10}$$

$$Y_t = Y_{t-1} + \alpha(\phi - Y_{t-1})\Delta t + \sigma_Y \Delta Z_t \tag{5.11}$$

where the two Brownian motions W_t and Z_t are correlated with a correlation ρ. Here, Δt is set to be $\frac{1}{260}$ where 260 is approximately the number of trading days in a year. The correlated Brownian motions W_t and Z_t can be sampled by first generating two sequences of independent standard normal distributed random numbers $\varepsilon_{1,t}$, $\varepsilon_{2,t}$. By performing a Cholesky decomposition, we further impose the correlation ρ on the independent series to obtain two sets of correlated random numbers $\varepsilon_{1,t}^c, \varepsilon_{2,t}^c$. By then, the paths for Brownian motions W_t and Z_t in equations (5.10)-(5.11) can be easily generated as follows:

$$\Delta W_t = \varepsilon_{1,t}^c \sqrt{\Delta t} \qquad \text{and} \qquad \Delta Z_t = \varepsilon_{2,t}^c \sqrt{\Delta t}.$$

Subsequently, we implement the updating functions (5.10)-(5.11) to compute the values of X and Y for any given times t. On each trading day, the log futures prices for different maturities are calculated by applying the known model parameter values, as well as the simulated values for log spot price and its mean level, to equation (5.1). For the purpose of our study, each futures curve is constructed to include 13 monthly contracts starting with the first contract maturing in 1 month and so forth, with the longest maturity contract expiring in 13 months. In Figure 5.1, we plot a simulated sample path of the log spot price and the stochastic mean level Y_t. Instead of plotting all the thirteen futures prices derived from the simulated path, three contract maturities, 3, 8, and 13-month log futures prices, are chosen to be illustrated in the figure. Interestingly, we observe that the simulated futures curves in Figure 5.1 maintain the well-known "Samuelson effect" which we mentioned in Chapter 2. For instance, it is apparent that the 13-month futures contract is less volatile than the 3-month futures since the former is less sensitive to the

noise in short term price fluctuations. Therefore, we have simulated the log spot and futures prices which allow us to proceed with investigating the robustness of the calibration procedure.
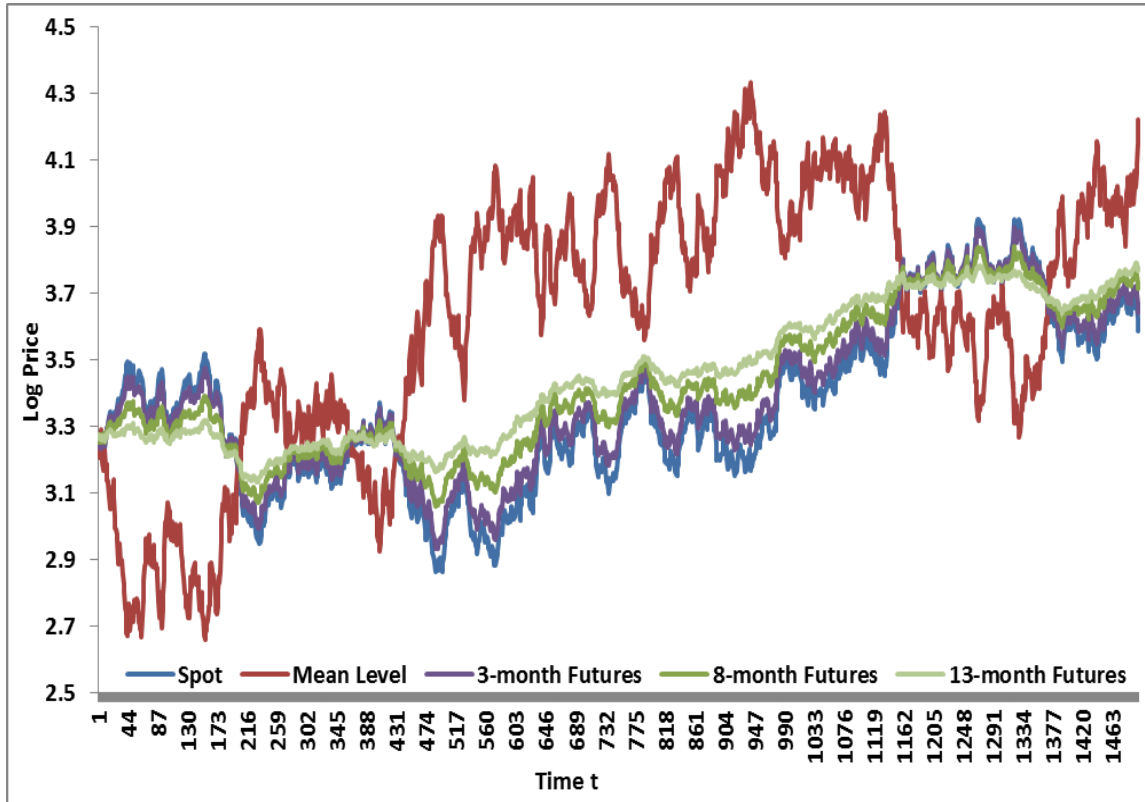
Figure 5.1 Log spot and futures prices simulated with the parameters in Table 5.1

5.4 Calibration Results and Sensitivity Analysis

In this section, we present the calibration results of implementing the HJ Model to our simulated data. For the purpose of our investigation, simulated data are preferred over actual data because we know that the simulated data are generated from the HJ Model with parameter values given in Table 5.1, without the concerns of whether the HJ Model provides a good description to the actual data. Moreover, our study mainly focuses on the

57

capability of the calibration procedure to discover the risk-neutral model parameters $(\bar{\beta}, \bar{\alpha}, \bar{\phi}, \sigma_X, \sigma_Y, \rho)$ from the simulated data. To estimate the risk-neutral parameters, we perform an optimization to obtain a set of parameters that minimizes the objective function (5.6). However, this optimization result might be very sensitive to different initial guesses for the model parameters. In other words, when initial guesses are set to be too far from the true values, the calibration results might not converge to the correct parameter values. Therefore, this problem has motivated us to further our research on this issue under the HJ framework.

Before we proceed to show the calibration results, it is useful for us to examine how changing parameter values will affect the value of our objective function. For each simulated path, we perform the so-called "one-factor-at-a-time" method whereby we move the value of a parameter within a reasonable range while keeping other parameters at their correct values. Using this new set of parameter values, we obtain the hidden long-run mean level Y_t from formula (5.5), and subsequently compute the sum of squared differences (SSE) between the simulated futures data and the calculated log futures prices, as described by equation (5.4). Then, we plot a curve of SSE with respect to the parameter values to gain understanding of the relationship between parameter values and the objective function. In Figure 5.2, we show the 5th, 95th percentile and mean SSE calculated for the 30 simulated paths while moving the values of $\bar{\alpha}$ in the range of 0 to 1. From the figure, we observe that the minimum value of SSE is achieved when alpha is equal to 0.15. This observation matches our expectation since the simulated data are generated with $\bar{\alpha} = 0.15$. Next, we repeat the same steps for $\bar{\beta}$ and Figure 5.3 illustrates the result that we have obtained. The graph shows that the SSE curve for every simulated
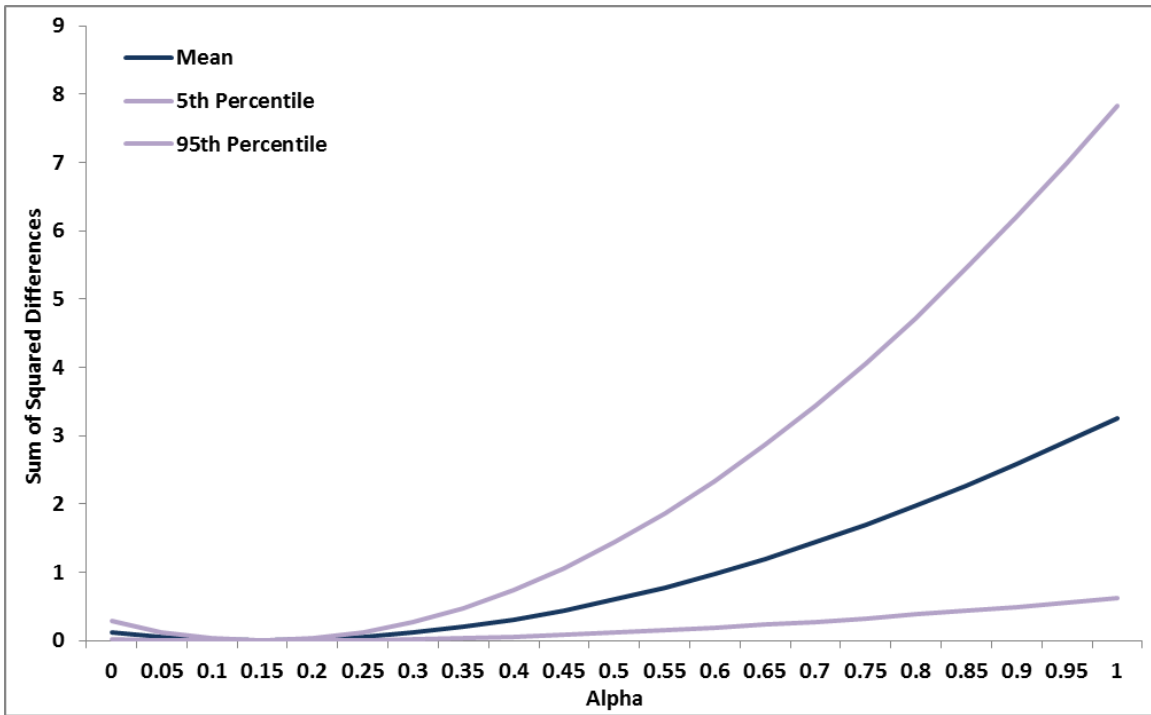
Figure 5.2 SSE curves with regard to changing values of $\bar{\alpha}$
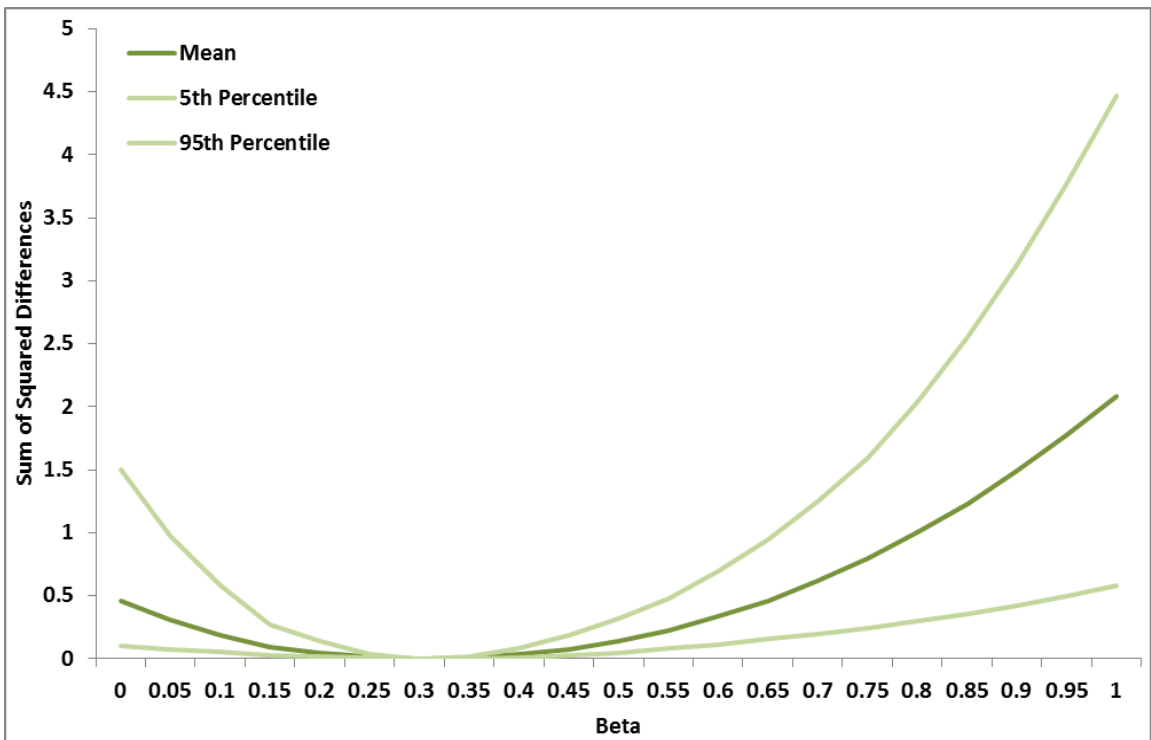
Figure 5.3 SSE curves with regard to changing values of $\bar{\beta}$

path can be described as a convex function with a global minimum point at $\bar{\beta} = 0.31$. Similar analyses are performed to the remaining 4 parameters and the results are displayed in Figures 5.4-5.7. Due to small deviations between the SSE curves for
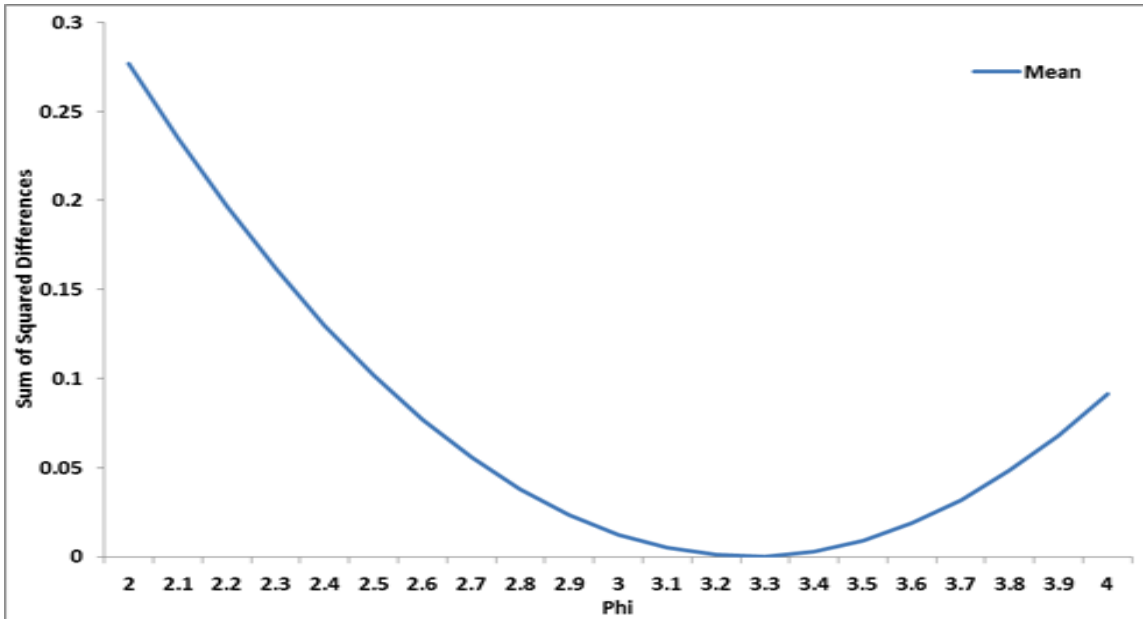
Figure 5.4 Mean SSE curve with regard to changing values of $\bar{\phi}$
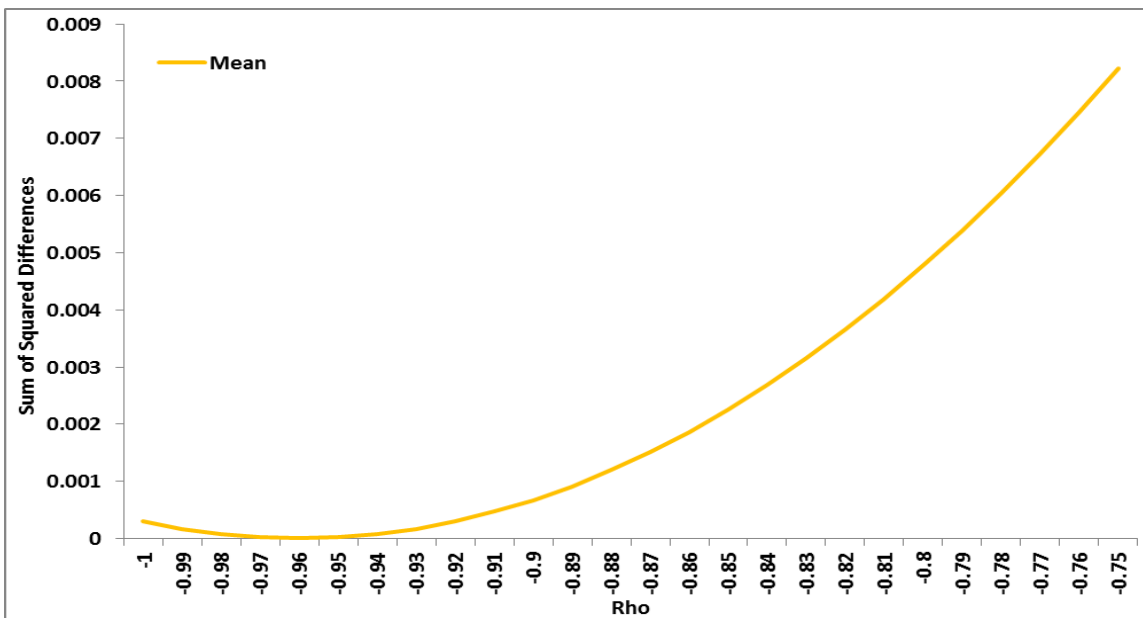
Figure 5.5 Mean SSE curve with regard to changing values of ρ
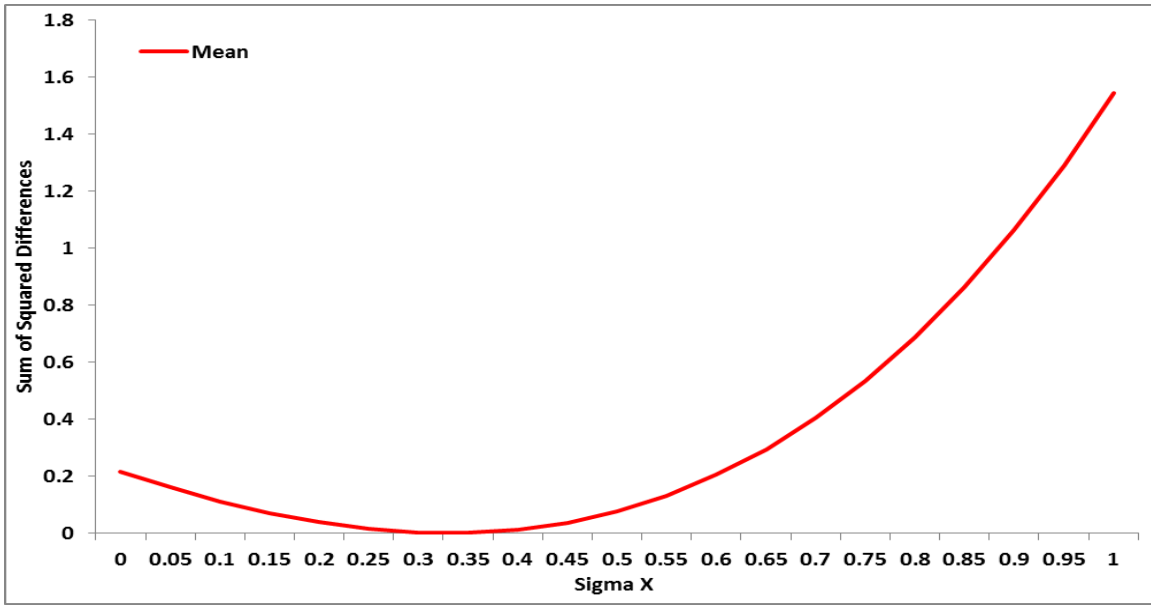
Figure 5.6 Mean SSE curve with regard to changing values of σ_X
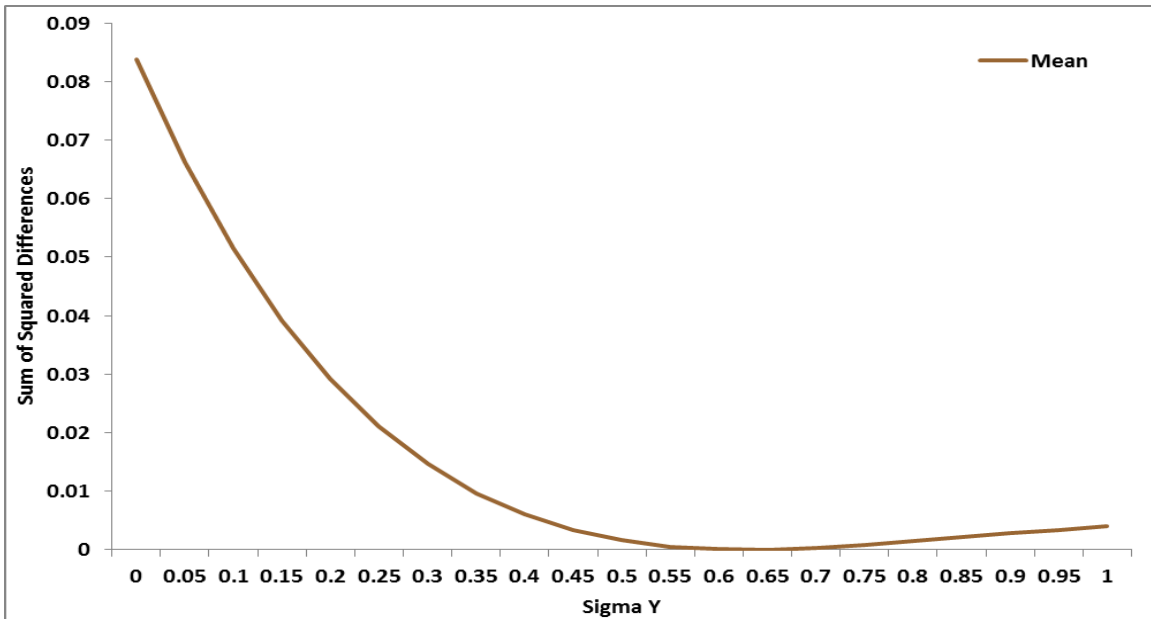
Figure 5.7 Mean SSE curve with regard to changing values of σ_Y

different simulated paths, we have only plotted the mean SSE curve for the parameters $\bar{\phi}$, ρ, σ_X and σ_Y. As expected, the results for these 4 parameters concur with our previous

findings for $\bar{\alpha}$ and $\bar{\beta}$, whereby the minimum value for SSE is attained with parameter values given in Table 5.1. Moreover, it is interesting to note that the mean SSE curve for σ_Y is relatively flat for values in between 0.5 and 1. This segment of the curve might suggest a potential problem for the optimization procedure to converge to the correct parameter value. After analyzing the SSE curves, we can be sure that when we are minimizing the objective function in the calibration procedure, we are in fact finding the parameter values that simulate these data. However, the "one-factor-at-a-time" approach does not fully explore all the possible outcomes because this method does not consider the simultaneous variation in the parameters. Therefore, this approach lacks the ability to identify the presence of interactions between parameters.

For the rest of this section, we will present the results of calibrating the HJ Model to our simulated data. Since the calibration process involves an optimization procedure, we are interested in investigating how different initial guesses for the parameter values can affect the calibration result. To solve the optimization problem in equation (5.6), we used the *lsqnonlin* function in Matlab. We begin by showing the calibration result of setting the initial guesses to the parameter values specified in Table 5.1. Table 5.2 shows the summary statistics of the optimal risk-neutral parameter values obtained from fitting

	$\bar{\alpha}$	$\bar{\beta}$	$\bar{\phi}$	ρ	σ_X	σ_Y	*RSS*	*Iterations*
True Value	0.15	0.31	3.27	-0.96	0.33	0.63		
Mean	0.15	0.31	3.27	-0.96	0.33	0.63	1.69E-14	0
Standard Deviation	0	1.13E-16	0	6.78E-16	0	2.26E-16	2.3E-15	0
Minimum	0.15	0.31	3.27	-0.96	0.33	0.63	1.38E-14	0
25th Percentile	0.15	0.31	3.27	-0.96	0.33	0.63	1.52E-14	0
75th Percentile	0.15	0.31	3.27	-0.96	0.33	0.63	1.79E-14	0
Maximum	0.15	0.31	3.27	-0.96	0.33	0.63	2.4E-14	0

Table 5.2 Calibration result by setting initial guesses to parameter value in Table 5.1

the HJ Model to our 30 simulated paths. For comparison, we also include the square-root of the sum of squares (RSS) for our estimated model and the number of iterations taken to achieve the optimized result. When parameter values in Table 5.1 are used as the initial guesses, it is not surprising to observe from Table 5.2 that all the optimal risk-neutral parameters remain at the correct values.

Next, we investigate the sensitivity of the calibration results by changing the initial guess of a single parameter while maintaining the others at their true values. For each parameter, we will examine the capability of the optimization process to produce unbiased parameter estimates when the initial guess is fixed at 20 percent away from its actual value. We start by looking at the calibration results that we have obtained when the initial guess of $\bar{\alpha}$ deviates from its true value. In Table 5.3, we show the estimated values of our model parameters when the initial guess of alpha is set to be 20% below its true value. In this case, the calibration process is able to produce parameter estimates which are very close to the actual values. Moreover, the parameter estimates attained for various simulated paths do not vary much and hence they have very low standard deviations. On average, the optimization process took 11.2 iterations to achieve the optimized result.[6]

	$\bar{\alpha}$	$\bar{\beta}$	$\bar{\phi}$	ρ	σ_X	σ_Y	RSS	Iterations
True Value	0.15	0.31	3.27	-0.96	0.33	0.63		
Mean	0.149971	0.310026	3.272392	-0.95808	0.331319	0.629047	6.47E-06	11.2
Standard Deviation	4.16E-05	3.54E-05	0.001631	0.002741	0.001068	0.000575	4.16E-06	4.25
Minimum	0.149787	0.31	3.270026	-0.96395	0.330019	0.627989	3.46E-07	7
25th Percentile	0.14995	0.310006	3.271077	-0.95997	0.330451	0.628552	3.39E-06	9
75th Percentile	0.149995	0.310045	3.273558	-0.956	0.331967	0.629565	9.72E-06	13
Maximum	0.15	0.310178	3.2764	-0.95122	0.334086	0.629782	1.94E-05	27

Table 5.3 Calibration result when initial guess of $\bar{\alpha}$ is set to be 0.12

---

[6] To prevent the optimization process from terminating prematurely, the maximum number of iterations allowed is 2000.

	$\bar{\alpha}$	$\bar{\beta}$	$\bar{\phi}$	ρ	σ_X	σ_Y	RSS	Iterations
True Value	0.15	0.31	3.27	-0.96	0.33	0.63		
Mean	0.150029	0.309974	3.276249	-0.95683	0.332926	0.627963	7.46E-06	14.1
Standard Deviation	4.67E-05	4E-05	0.006561	0.006171	0.003359	0.002282	4.38E-06	5.82
Minimum	0.149981	0.309834	3.26568	-0.96439	0.328184	0.623736	1.12E-06	7
25th Percentile	0.150004	0.309967	3.271359	-0.9612	0.33047	0.626019	4.69E-06	10
75th Percentile	0.150035	0.31	3.281223	-0.95116	0.33566	0.629669	9.79E-06	16.5
Maximum	0.1502	0.310022	3.288037	-0.94313	0.340521	0.631423	1.92E-05	31

Table 5.4 Calibration result when initial guess of $\bar{\alpha}$ is set to be 0.18

Subsequently, we change the initial guess of alpha to be 20% above its true value and the calibration result is displayed in Table 5.4. Similarly, the differences between the mean estimates and the actual values are relatively small for all the model parameters. Hence, when the initial guess of alpha is 20% apart from its true value, the calibration process can provide very accurate estimates of the model parameters. To extend our investigation, we include initial guesses of alpha which are further apart from its actual value. As presented in Table 5.5, a very similar result is obtained from the calibration process when the initial guess of $\bar{\alpha}$ is 0. However, approximately 10% of the results show slightly more obvious deviations between the actual values and the estimates of ρ and σ_X. To complete our investigation for alpha, we ran the calibration process with an initial guess of 1. In Table 5.6, all of the model parameters have obvious differences between their mean

	$\bar{\alpha}$	$\bar{\beta}$	$\bar{\phi}$	ρ	σ_X	σ_Y	RSS	Iterations
True Value	0.15	0.31	3.27	-0.96	0.33	0.63		
Mean	0.149973	0.310025	3.282222	-0.94964	0.337004	0.625489	9.12E-06	16.4
Standard Deviation	4.31E-05	3.68E-05	0.011156	0.01170	0.006436	0.004002	5.51E-06	7.27
Minimum	0.149813	0.309998	3.263983	-0.96416	0.328453	0.617344	1.03E-06	7
25th Percentile	0.149973	0.310005	3.275638	-0.95915	0.332036	0.62261	4.82E-06	12
75th Percentile	0.149995	0.310024	3.288406	-0.93999	0.342357	0.628003	1.43E-05	18.75
Maximum	0.150002	0.310159	3.307216	-0.92214	0.349909	0.63165	2.08E-05	42

Table 5.5 Calibration result when initial guess of $\bar{\alpha}$ is set to be 0

	$\bar{\alpha}$	$\bar{\beta}$	$\bar{\phi}$	ρ	σ_X	σ_Y	RSS	Iterations
True Value	0.15	0.31	3.27	-0.96	0.33	0.63		
Mean	0.18846	0.27164	3.22202	-0.94362	0.46194	0.75772	0.00122	60
Standard Deviation	0.066	0.06594	0.28864	0.04057	0.30827	0.15953	0.00295	64.75
Minimum	0.14997	0.15552	2.38643	-1	0.11467	0.54277	3.9E-06	18
25th Percentile	0.15001	0.25084	3.02692	-0.96708	0.26086	0.63076	0.00004	26.25
75th Percentile	0.21116	0.30999	3.4631	-0.91435	0.43529	0.9624	0.00157	51.75
Maximum	0.30454	0.31003	3.61279	-0.84955	1	1	0.0155	272

Table 5.6 Calibration result when initial guess of $\bar{\alpha}$ is set to be 1

estimates and the true values. This outcome is influenced by a few estimation results that are unsuccessful in providing accurate estimates of the model parameters. Figure 5.8 suggests that, out of the 30 sample paths, more than 25% of the optimized results failed to converge to the true value of alpha. The reason may be that the standard local optimizer
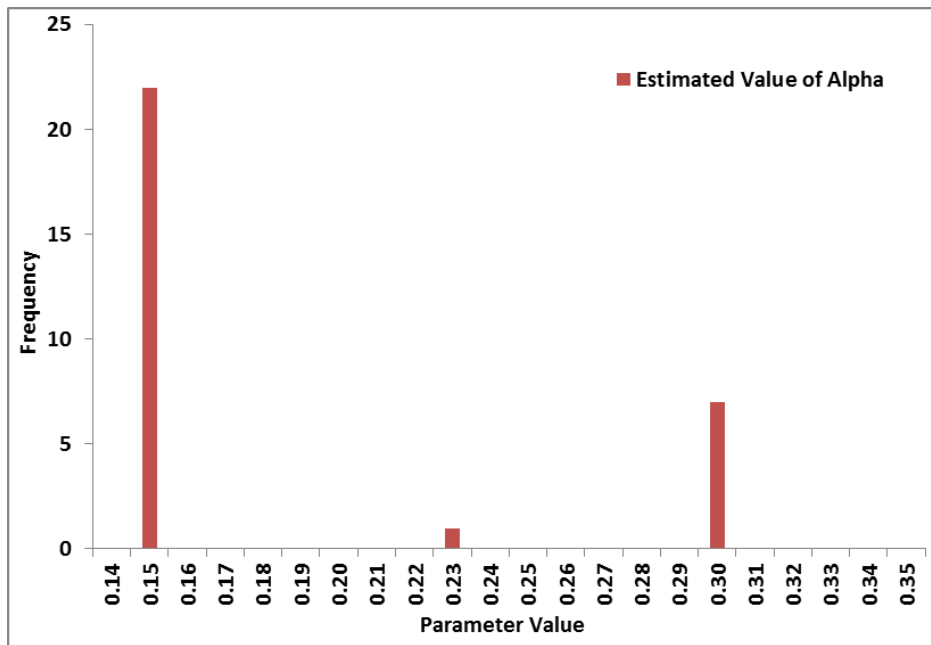
Figure 5.8 Histogram of estimated values of alpha when initial guess is 1

used here stops in the local minima at $\bar{\alpha} = 0.23$ and 0.30 instead of proceeding further to reach the global minimum. Furthermore, when the value of $\bar{\alpha}$ is inaccurately estimated,

the estimation for other parameters will also be affected, as described in Table 5.7:

$\bar{\alpha}$	$\bar{\beta}$	$\bar{\phi}$	ρ	σ_X	σ_Y	RSS
0.3031	0.1569	3.5777	-0.9941	1	1	0.0028
0.2315	0.2312	3.0475	-0.8734	0.2977	1	0.0155

Table 5.7 Calibration result when estimates of $\bar{\alpha}$ deviates from its true value

However, we can easily distinguish these results from those obtained under global minimum since the RSS values in Table 5.7 are significantly greater than those seen in Table 5.3. Therefore, looking at all the results obtained by changing the initial guesses of alpha, we discover that the calibration procedure is very robust in providing accurate estimates of the model parameters. A few exceptions apply when the initial guesses are set to deviate too far from the true value, which might cause the optimization algorithm to get stuck in local minima.

We continue our analysis and study the calibration results when the initial guesses of $\bar{\beta}$ are specified to differ from its true value. Table 5.8 and Table 5.9 respectively show the estimation results when the initial values of beta are assigned to be 20% smaller and 20% larger than the actual value. These results reaffirm the ability of the calibration process to obtain very stable yet accurate parameter estimates when the initial guesses of

	$\bar{\alpha}$	$\bar{\beta}$	$\bar{\phi}$	ρ	σ_X	σ_Y	RSS	Iterations
True Value	0.15	0.31	3.27	-0.96	0.33	0.63		
Mean	0.150023	0.30998	3.274188	-0.96031	0.331261	0.62875	5.4E-06	11.83
Standard Deviation	3.26E-05	2.81E-05	0.002439	0.00591	0.002319	0.000979	3.52E-06	3.7
Minimum	0.149996	0.309854	3.270164	-0.97276	0.327857	0.626727	7.71E-07	8
25th Percentile	0.150003	0.309969	3.272129	-0.96513	0.32898	0.628081	2.74E-06	9
75th Percentile	0.150033	0.309997	3.276111	-0.95838	0.332307	0.629581	7.08E-06	13
Maximum	0.150171	0.310005	3.27798	-0.94152	0.337821	0.630245	1.81E-05	22

Table 5.8 Calibration result when initial guess of $\bar{\beta}$ is set to be 0.248

	$\bar{\alpha}$	$\bar{\beta}$	$\bar{\phi}$	ρ	σ_X	σ_Y	RSS	Iterations
True Value	0.15	0.31	3.27	-0.96	0.33	0.63		
Mean	0.149976	0.310021	3.274844	-0.95933	0.331754	0.628335	6.0E-06	13.57
Standard Deviation	4.09E-05	3.49E-05	0.006375	0.00452	0.002563	0.002066	4.05E-06	5.71
Minimum	0.149815	0.31	3.267043	-0.97290	0.328371	0.623243	9.34E-07	8
25th Percentile	0.149979	0.310003	3.269538	-0.96214	0.329652	0.627286	3.56E-06	10.25
75th Percentile	0.149997	0.310021	3.278025	-0.95733	0.333246	0.630046	7.54E-06	15
Maximum	0.15	0.310157	3.290853	-0.94943	0.337394	0.631042	1.91E-05	39

Table 5.9 Calibration result when initial guess of $\bar{\beta}$ is set to be 0.372

$\bar{\beta}$ are set to deviate 20% from the true value. To test the calibration technique to a greater extent, we change the initial guess of beta to 0. The result obtained under this setting is presented in Table 5.10. We observe some small differences between the mean estimates of the parameters and their actual values. This is mainly affected by 2 estimation results that eventually get stuck in local minima without proceeding to find the true parameter values at the global minimum. In fact, the estimation results for these 2 cases are identical to the parameter estimates which we have presented in the first row of Table 5.7. Next,

	$\bar{\alpha}$	$\bar{\beta}$	$\bar{\phi}$	ρ	σ_X	σ_Y	RSS	Iterations
True Value	0.15	0.31	3.27	-0.96	0.33	0.63		
Mean	0.160312	0.299689	3.331837	-0.93284	0.398685	0.638618	0.000247	24.83
Standard Deviation	0.039148	0.039154	0.084448	0.02695	0.165574	0.100563	0.000837	16.83
Minimum	0.149997	0.155492	3.228619	-0.99998	0.318886	0.543694	4.93E-06	12
25th Percentile	0.150003	0.309961	3.264625	-0.94504	0.33378	0.599493	1.2E-05	15
75th Percentile	0.150042	0.309997	3.359234	-0.91365	0.377499	0.634218	4.0E-05	26
Maximum	0.304564	0.310004	3.555267	-0.87978	1	1	0.003389	88

Table 5.10 Calibration result when initial guess of $\bar{\beta}$ is set to be 0

we assigned the initial guess of $\bar{\beta}$ to 1 and Table 5.11 summarizes the calibration results. The calibration process is able to provide very stable and accurate estimates of $\bar{\alpha}$ and $\bar{\beta}$, with negligible differences between the mean estimates and their true values. On the

other hand, we observe that the mean estimates for the remaining four parameters are slightly deviated from their actual values. Despite that, we find the calibration technique

	$\bar{\alpha}$	$\bar{\beta}$	$\bar{\phi}$	ρ	σ_X	σ_Y	RSS	Iterations
True Value	0.15	0.31	3.27	-0.96	0.33	0.63		
Mean	0.149969	0.310028	3.305852	-0.91534	0.356856	0.615028	2.83E-05	21.33
Standard Deviation	4.72E-05	4.02E-05	0.069149	0.04416	0.034082	0.025115	2.41E-05	8.71
Minimum	0.149811	0.309997	3.21657	-0.98195	0.320703	0.555497	6.0E-06	11
25th Percentile	0.149963	0.310003	3.252355	-0.95177	0.330532	0.601738	1.21E-05	15
75th Percentile	0.149997	0.310034	3.33836	-0.89258	0.372899	0.634724	3.82E-05	24.75
Maximum	0.150004	0.31016	3.460895	-0.81731	0.441023	0.645373	9.22E-05	49

Table 5.11 Calibration result when initial guess of $\bar{\beta}$ is set to be 1

to be capable of giving relatively good estimates of the model parameters when the initial guesses of $\bar{\beta}$ deviate from its true value.

We proceed to examine the robustness of the calibration process when the initial guesses of $\bar{\phi}$ deviate from its actual value. Table 5.12 contains the calibration result obtained by setting the initial guess of $\bar{\phi}$ to be 20% less than its true value. We discover the estimations of $\bar{\alpha}$ and $\bar{\beta}$ remain at the correct values while the calibrated values of $\bar{\phi}$, ρ, σ_X and σ_Y are significantly changed from their true values. On average, there is a 10-percent difference between the estimated value of $\bar{\phi}$ and its correct value. Moreover,

	$\bar{\alpha}$	$\bar{\beta}$	$\bar{\phi}$	ρ	σ_X	σ_Y	RSS	Iterations
True Value	0.15	0.31	3.27	-0.96	0.33	0.63		
Mean	0.149979	0.310019	2.941667	-0.79983	0.277421	0.718631	0.000108	13.87
Standard Deviation	4.0E-05	3.47E-05	0.021615	0.01414	0.003636	0.005336	7.08E-06	5.94
Minimum	0.149804	0.30999	2.907939	-0.81534	0.270247	0.708177	9.46E-05	7
25th Percentile	0.149982	0.310002	2.920478	-0.80913	0.274712	0.715732	0.0001	10
75th Percentile	0.149998	0.310015	2.953854	-0.79075	0.278918	0.723452	0.000115	15.75
Maximum	0.15001	0.310166	2.982169	-0.7683	0.285861	0.727063	0.000119	33

Table 5.12 Calibration result when initial guess of $\bar{\phi}$ is set to be 2.616

we note that when estimation of $\bar{\phi}$ fails to converge to the correct value, it is very likely for us to also get inaccurate calibrated values for parameters ρ, σ_X and σ_Y. This observation might suggest the presence of interactions among the four parameters. When

	$\bar{\alpha}$	$\bar{\beta}$	$\bar{\phi}$	ρ	σ_X	σ_Y	RSS	Iterations
True Value	0.15	0.31	3.27	-0.96	0.33	0.63		
Mean	0.15001	0.309989	3.524731	-0.98590	0.414038	0.541219	0.00011	22.83
Standard Deviation	3.56E-05	4.62E-05	0.017252	0.01446	0.006385	0.006535	4.82E-05	36.47
Minimum	0.149973	0.309754	3.480792	-1	0.401687	0.523255	8.61E-05	9
25th Percentile	0.149997	0.309992	3.514185	-0.99725	0.410253	0.539271	9.86E-05	12
75th Percentile	0.15001	0.310004	3.530905	-0.97140	0.415734	0.544296	0.000103	16
Maximum	0.150183	0.310027	3.56764	-0.95638	0.432818	0.556242	0.000363	200

Table 5.13 Calibration result when initial guess of $\bar{\phi}$ is set to be 3.924

the initial guess of $\bar{\phi}$ is set to be 20% above its true value, the calibration result with a similar pattern is discovered in Table 5.13, whereby the optimization process fails to recover the original parameter values for $\bar{\phi}$, ρ, σ_X and σ_Y. To test whether initial guesses which are closer to the actual value can improve the calibration result, Table 5.14 and Table 5.15 respectively summarize the estimation results obtained by setting the initial guesses of $\bar{\phi}$ as 10% smaller and 10% larger than its true value. Even though differences between the estimated values and the actual values of $\bar{\phi}$, ρ, σ_X and σ_Y have become

	$\bar{\alpha}$	$\bar{\beta}$	$\bar{\phi}$	ρ	σ_X	σ_Y	RSS	Iterations
True Value	0.15	0.31	3.27	-0.96	0.33	0.63		
Mean	0.149989	0.310011	3.116857	-0.88814	0.303358	0.673216	5.2E-05	12.17
Standard Deviation	5.06E-05	4.35E-05	0.010106	0.01188	0.001601	0.002504	2.52E-06	4.04
Minimum	0.149917	0.3098	3.089511	-0.92728	0.299909	0.668195	4.84E-05	7
25th Percentile	0.149976	0.310005	3.113734	-0.88712	0.302247	0.671539	5.0E-05	10
75th Percentile	0.149995	0.310024	3.12228	-0.88439	0.304324	0.67411	5.25E-05	14.75
Maximum	0.150235	0.310071	3.142058	-0.86392	0.305975	0.680161	6.0E-05	27

Table 5.14 Calibration result when initial guess of $\bar{\phi}$ is set to be 2.943

	$\bar{\alpha}$	$\bar{\beta}$	$\bar{\phi}$	ρ	σ_X	σ_Y	RSS	Iterations
True Value	0.15	0.31	3.27	-0.96	0.33	0.63		
Mean	0.15001	0.309992	3.41589	-0.9766	0.37471	0.581841	5.64E-05	11.33
Standard Deviation	2.55E-05	2.18E-05	0.010891	0.00903	0.005602	0.004132	5.0E-06	4.54
Minimum	0.149964	0.309906	3.396909	-0.99207	0.363076	0.573205	4.68E-05	5
25th Percentile	0.15	0.30999	3.408786	-0.9874	0.37028	0.579383	5.19E-05	9
75th Percentile	0.150011	0.31	3.422479	-0.97025	0.378571	0.585152	5.93E-05	12.75
Maximum	0.150113	0.310035	3.441694	-0.96612	0.383157	0.589465	6.61E-05	28

Table 5.15 Calibration result when initial guess of $\bar{\phi}$ is set to be 3.597

smaller, the calibration process still fails to converge to the correct values for these parameters. These results suggest that the optimization process is likely trapped inside a flat region around the global minimum. Therefore, it is not surprising for us to observe from Table 5.16 that the estimates for these four parameters are largely deviated from their true values when the initial guess of $\bar{\phi}$ is chosen to be 2. We conclude that the

	$\bar{\alpha}$	$\bar{\beta}$	$\bar{\phi}$	ρ	σ_X	σ_Y	RSS	Iterations
True Value	0.15	0.31	3.27	-0.96	0.33	0.63		
Mean	0.149989	0.310009	2.677859	-0.64862	0.246402	0.780784	0.000191	14.2
Standard Deviation	1.56E-05	1.42E-05	0.050059	0.01865	0.012516	0.011835	1.69E-05	3.96
Minimum	0.149939	0.309996	2.588086	-0.67292	0.218425	0.76255	0.000166	9
25th Percentile	0.149987	0.309999	2.639859	-0.66451	0.240441	0.7685	0.000173	11.25
75th Percentile	0.150001	0.310012	2.730858	-0.63493	0.257152	0.78942	0.00020	15
Maximum	0.150003	0.31005	2.753491	-0.61175	0.264191	0.802253	0.000222	26

Table 5.16 Calibration result when initial guess of $\bar{\phi}$ is set to be 2

calibration technique is unsuccessful in providing the correct parameter estimates for $\bar{\phi}$, ρ, σ_X and σ_Y even when the initial guesses of $\bar{\phi}$ are set in close proximity to the actual value. Moreover, the presence of interactions among these four parameters might be the reason why the estimates of ρ, σ_X and σ_Y are also inaccurate when the initial guess of $\bar{\phi}$ deviates from its correct value.

As we can see from Table 5.17, the calibration process is once again having difficulty estimating the correct parameter values of $\bar{\phi}$, ρ, σ_X and σ_Y, when the initial guess of ρ is set to be 20% larger than its true value. In this case, the calibrated values of ρ are hugely deviated from its actual value, with an average estimation error of 17%. Moreover, the results in Table 5.17 also reaffirm our hypothesis that interactions might exist among these four parameters. In hopes of improving the accuracy of the calibration result, we assign the initial guess of ρ to have a 10% deviation from the true value.

	$\bar{\alpha}$	$\bar{\beta}$	$\bar{\phi}$	ρ	σ_X	σ_Y	RSS	Iterations
True Value	0.15	0.31	3.27	-0.96	0.33	0.63		
Mean	0.149996	0.310003	3.193902	-0.78989	0.359218	0.645244	1.36E-05	8.97
Standard Deviation	2.74E-05	2.5E-05	0.006839	0.00668	0.004634	0.002577	3.0E-06	2.58
Minimum	0.149918	0.309953	3.181236	-0.8025	0.350495	0.638294	7.9E-06	5
25th Percentile	0.149979	0.309987	3.189671	-0.79531	0.355847	0.643669	1.15E-05	7.25
75th Percentile	0.150014	0.310018	3.197984	-0.78631	0.361875	0.64693	1.5E-05	10.75
Maximum	0.150051	0.310071	3.212065	-0.77256	0.371756	0.650025	1.92E-05	15

Table 5.17 Calibration result when initial guess of ρ is set to be -0.768

	$\bar{\alpha}$	$\bar{\beta}$	$\bar{\phi}$	ρ	σ_X	σ_Y	RSS	Iterations
True Value	0.15	0.31	3.27	-0.96	0.33	0.63		
Mean	0.149985	0.310012	3.233207	-0.87176	0.344748	0.637323	9.0E-06	9.2
Standard Deviation	5.36E-05	4.63E-05	0.006222	0.00411	0.003352	0.002221	4.1E-06	4.24
Minimum	0.149802	0.309932	3.220414	-0.87946	0.338118	0.632293	3.22E-06	4
25th Percentile	0.149979	0.309991	3.229481	-0.87495	0.342286	0.63649	5.85E-06	6
75th Percentile	0.150008	0.310019	3.235249	-0.87049	0.345782	0.638904	1.05E-05	11
Maximum	0.150077	0.310168	3.247476	-0.86245	0.352491	0.641759	2.09E-05	21

Table 5.18 Calibration result when initial guess of ρ is set to be -0.864

However, Table 5.18 demonstrates that this initial input still does not facilitate the optimization process to recover all the correct parameter values. In fact, none of the

calibration results given in Table 5.19 can precisely estimate the parameter value of ρ, even when the initial guess is set to -1 which is pretty close to the true value. By

	$\bar{\alpha}$	$\bar{\beta}$	$\bar{\phi}$	ρ	σ_X	σ_Y	RSS	Iterations
True Value	0.15	0.31	3.27	-0.96	0.33	0.63		
Mean	0.150007	0.309993	3.286527	-0.99082	0.3266	0.626145	5.14E-06	6.37
Standard Deviation	1.38E-05	1.25E-05	0.000655	0.00132	0.000171	0.000126	1.56E-06	2.16
Minimum	0.149978	0.30997	3.284555	-0.99218	0.326482	0.625862	3.35E-06	4
25th Percentile	0.15	0.309986	3.286604	-0.99141	0.326508	0.626082	3.75E-06	5
75th Percentile	0.150014	0.31	3.286845	-0.99121	0.326558	0.62618	6.32E-06	7.75
Maximum	0.150035	0.31002	3.287661	-0.98696	0.327046	0.62648	8.8E-06	11

Table 5.19 Calibration result when initial guess of ρ is set to be -1

comparing the RSS values in Table 5.19 with those in Table 5.17, we may infer that the differences between these values are quite insignificant. Hence, it is very likely that the optimization algorithm is again trapped inside a wide and flat valley, without being able to move forward to reach the global minimum.

We perform similar analyses for parameter σ_X and calibration results that resemble our previous observations for ρ are obtained. As presented in Table 5.20 and Table 5.21, the calibration process fails to recover the correct parameter values of $\bar{\phi}$, ρ, σ_X and σ_Y, when the initial guesses of σ_X are respectively set to deviate by 20% and 10%

	$\bar{\alpha}$	$\bar{\beta}$	$\bar{\phi}$	ρ	σ_X	σ_Y	RSS	Iterations
True Value	0.15	0.31	3.27	-0.96	0.33	0.63		
Mean	0.150011	0.309991	3.35921	-0.91187	0.37501	0.597913	4.06E-05	10.03
Standard Deviation	2.52E-05	2.26E-05	0.001492	0.00284	0.000621	0.000359	6.08E-07	2.58
Minimum	0.149959	0.309927	3.356571	-0.91877	0.373722	0.597125	4.0E-05	4
25th Percentile	0.15	0.309981	3.358654	-0.91315	0.374649	0.597753	4.0E-05	9
75th Percentile	0.15002	0.310001	3.360337	-0.91135	0.375436	0.598174	4.1E-05	11.75
Maximum	0.150087	0.310043	3.361969	-0.905	0.376592	0.598475	4.23E-05	16

Table 5.20 Calibration result when initial guess of σ_X is set to be 0.396

	$\bar{\alpha}$	$\bar{\beta}$	$\bar{\phi}$	ρ	σ_X	σ_Y	RSS	Iterations
True Value	0.15	0.31	3.27	-0.96	0.33	0.63		
Mean	0.150012	0.30999	3.315731	-0.93452	0.352595	0.613976	2.1E-05	9.27
Standard Deviation	3.39E-05	3E-05	0.000939	0.0018	0.000293	0.000168	1.18E-06	2.89
Minimum	0.149942	0.309877	3.313331	-0.93707	0.35225	0.613636	2.0E-05	5
25th Percentile	0.15	0.309979	3.315605	-0.93537	0.352431	0.613899	2.0E-05	7
75th Percentile	0.150022	0.31	3.316251	-0.93486	0.352663	0.614033	2.14E-05	11
Maximum	0.150143	0.310055	3.317177	-0.9293	0.353627	0.614332	2.55E-05	18

Table 5.21 Calibration result when initial guess of σ_X is set to be 0.363

from the true value. Lastly, we proceed to examine how different selections of initial guesses for σ_Y can affect the calibration results. Table 5.22 summarizes the estimation result obtained by setting the initial guess to deviate by 20% from its true value. In this case, the calibration process still has not managed to provide accurate estimates for $\bar{\phi}$, ρ,

	$\bar{\alpha}$	$\bar{\beta}$	$\bar{\phi}$	ρ	σ_X	σ_Y	RSS	Iterations
True Value	0.15	0.31	3.27	-0.96	0.33	0.63		
Mean	0.149969	0.310028	3.321645	-0.96193	0.346301	0.61329	2.13E-05	14.4
Standard Deviation	4.38E-05	3.73E-05	0.008983	0.00301	0.003558	0.003054	4.19E-06	5.79
Minimum	0.149822	0.310001	3.300247	-0.96823	0.337376	0.609369	1.15E-05	8
25th Percentile	0.149956	0.310006	3.320001	-0.96283	0.345702	0.611362	1.94E-05	10.25
75th Percentile	0.149995	0.31004	3.327569	-0.95958	0.348332	0.613929	2.34E-05	17
Maximum	0.15	0.310151	3.333525	-0.95691	0.350145	0.620679	2.74E-05	33

Table 5.22 Calibration result when initial guess of σ_Y is set to be 0.504

	$\bar{\alpha}$	$\bar{\beta}$	$\bar{\phi}$	ρ	σ_X	σ_Y	RSS	Iterations
True Value	0.15	0.31	3.27	-0.96	0.33	0.63		
Mean	0.149921	0.310074	3.832744	-0.99527	0.601644	0.362151	0.000281	22.93
Standard Deviation	0.000138	0.000127	0.02641	0.01103	0.030264	0.027503	2.41E-05	7.23
Minimum	0.149526	0.309999	3.790345	-1	0.555629	0.311338	0.000242	8
25th Percentile	0.149946	0.310011	3.809432	-0.99999	0.573566	0.342458	0.00026	18
75th Percentile	0.149991	0.310053	3.854081	-0.99729	0.62299	0.385606	0.0003	25
Maximum	0.150002	0.310459	3.874108	-0.95573	0.658384	0.403054	0.000324	43

Table 5.23 Calibration result when initial guess of σ_Y is set to be 0

σ_X, and σ_Y, even though the estimation errors between the calibrated values and the actual values have become significantly smaller. To magnify the problem, we can set the initial guess of σ_Y to 0. From Table 5.23, we observe that the estimates for these four parameters are widely deviated from their actual values. We suspect that this outcome is mainly caused by our standard optimization method which tends to find a local minimum in the flat region and terminates before reaching the global minimum. Overall, we conclude that the calibration procedure is capable of providing very stable and accurate estimates of $\bar{\alpha}$ and $\bar{\beta}$. On the other hand, the method has a lot of difficulty in estimating the correct parameter values of $\bar{\phi}, \rho, \sigma_X$, and σ_Y, when their initial guesses are deviated from their respective true values. With the presence of interactions among these parameters, the ability to accurately estimate one of the parameters will also greatly depend on the initial guesses of the other parameters.

Realistically, we will never know the true parameter values which best describe an empirical dataset before performing a calibration procedure. Therefore, it is difficult to determine the appropriate values to use as initial guesses for the optimization process and whether these values can lead to convergence to the true parameter values. Moreover, we should not rely solely on a single calibration result obtained with a particular set of initial guesses since the optimization results might be very sensitive to the selections of initial guesses. To imitate better the problems we might face in reality, we make a few modifications to our previous investigations. For each model parameter, we specify a reasonable range of values in which the true parameter value is likely to fall. By using uniformly distributed random numbers, we arbitrarily select initial guesses for all the parameters from their respective ranges. Then, the calibration procedure is performed

multiple times on the same simulated path by applying distinctive sets of initial guesses. Since we only have one empirical price process in real life, this analysis will help us to gain an insight into how calibration results attained from the same data series can be affected by various selections of initial guesses. Table 5.24 summarizes the estimation results obtained after applying the calibration method with 200 different sets of randomly

	$\bar{\alpha}$	$\bar{\beta}$	$\bar{\phi}$	ρ	σ_X	σ_Y	RSS	Iterations
True Value	0.15	0.31	3.27	-0.96	0.33	0.63		
Mean	0.17897	0.28112	3.32226	-0.52874	0.70739	0.59982	0.001	79.54
Standard Deviation	0.06097	0.06077	0.32529	0.31061	0.22188	0.24874	0.00169	249.07
Minimum	0.14999	0.15366	2.45818	-1	0.23499	0.07115	1.1E-06	8
25th Percentile	0.15	0.31	3.09912	-0.79163	0.51819	0.44321	0.0001	15
75th Percentile	0.15	0.31	3.50773	-0.27013	0.92436	0.74375	0.00045	29
Maximum	0.30682	0.31001	3.81882	0.09377	1	1	0.00802	2000

Table 5.24 Calibration results obtained from a simulated path after performing optimization with 200 distinctive sets of random initial guesses

selected initial guesses. As we can see, all the mean estimates for the model parameters are significantly biased from their respective true values. Moreover, we note that there are two instances whereby the optimization process fails to converge to a solution after 2000 iterations. To have a better picture of the estimation results, we plotted histograms of the calibrated values for each risk-neutral parameter in Figure 5.9. We observe that the calibration process only produces two possible outcomes for the estimations of $\bar{\alpha}$ and $\bar{\beta}$, which is either "$\bar{\alpha} = 0.15 \ and \ \bar{\beta} = 0.31$" or "$\bar{\alpha} = 0.31 \ and \ \bar{\beta} = 0.15$". Out of the two possible results, there is an 18% chance that the latter combination of parameter estimates, which widely deviate from the true values, could be provided by the optimization process. As mentioned before, this outcome is obtained from the local minima since the optimization method fails to reach the global minimum, when selections of initial guesses
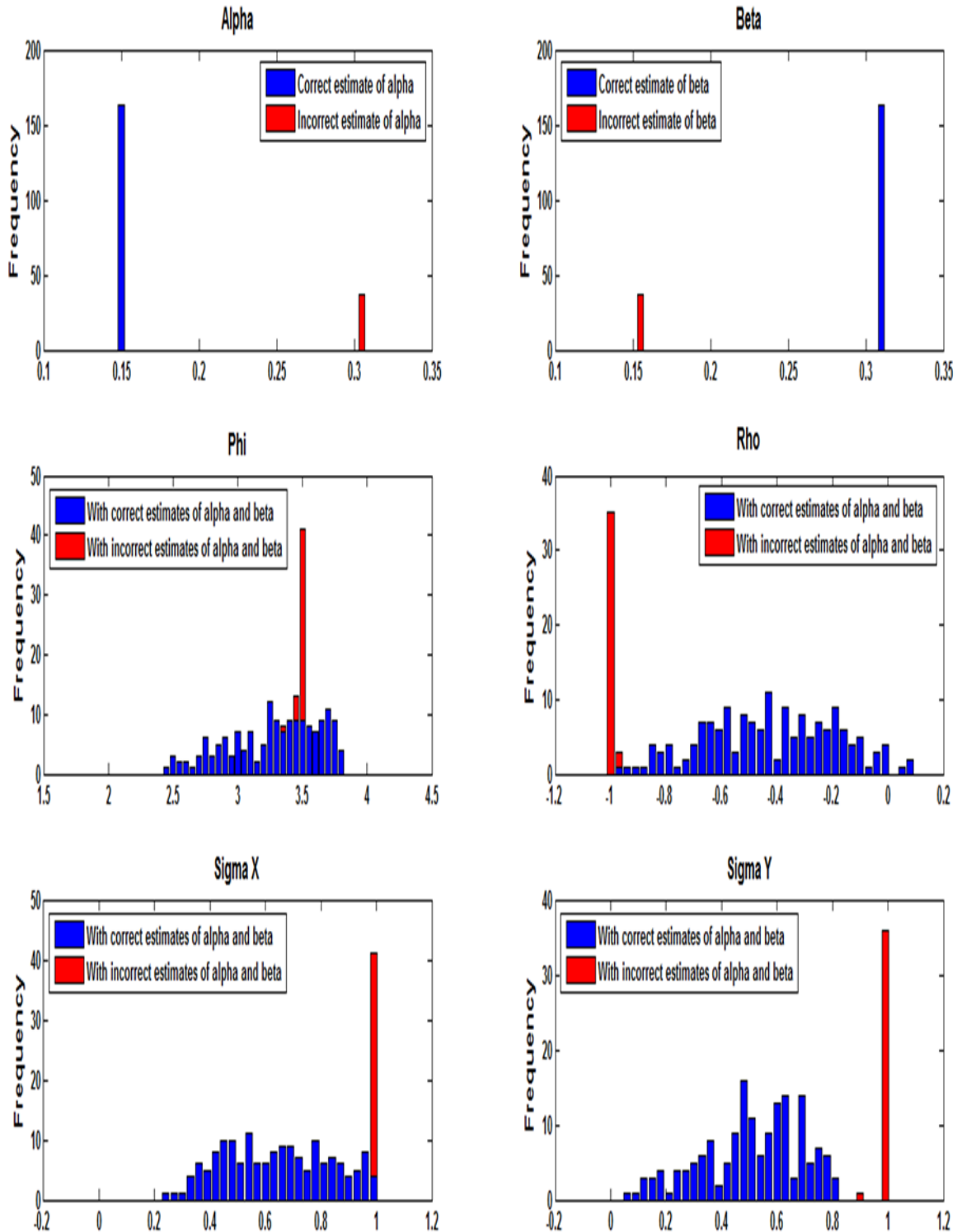
Figure 5.9 Histograms of estimated parameter values when calibration is performed on a simulated path with 200 distinctive sets of random initial guesses. Blue-colored bars correspond to the correct estimates of $\bar{\alpha}$ and $\bar{\beta}$, while red-colored bars correspond to incorrect estimates of $\bar{\alpha}$ and $\bar{\beta}$.

are far from the true values. However, we can easily distinguish the accurate parameter estimates from the local optimums because the SSE values given by the latter are significantly greater than those obtained at global minimum. Another interesting phenomenon noticed is that the estimated values of $\bar{\alpha}$ and $\bar{\beta}$ from one of the possible outcomes appear to be the reverse of the other, that is, the $\bar{\alpha}$ of one outcome has the same value as the $\bar{\beta}$ of the other and vice versa. This implies the estimation of one parameter is strongly dependent on the estimation of the other and may suggest the presence of interaction between $\bar{\alpha}$ and $\bar{\beta}$. Proceeding to the estimation of $\bar{\phi}$, we observe that the calibrated values lie within the interval of 2.45 and 3.8, with the highest frequency at $\bar{\phi} = 3.5$. Even though a lot of the calibration results of $\bar{\phi}$ cluster around the value of 3.5, these results can be misleading for someone to think that the highest frequency in the histogram is exactly where the true parameter value lies. Moreover, judging from the lack of significant differences between the SSE values calculated from various estimations of $\bar{\phi}$, we cannot easily identify which calibrated value is actually the best estimate for this parameter. Therefore, without knowing the true values of $\bar{\phi}$, we can only conclude that there is a high probability that the true value lies within the interval [2.45, 3.8], and all parameter values in this range are equally possible to become the best estimate of $\bar{\phi}$. Similar situations are observed for other parameters, namely ρ, σ_X and σ_Y, whereby the estimations of these parameters are provided by a range of possible values.

One speculation to help explain this observation is that the gradient-based optimization algorithm might have difficulties in finding the global minimum when it is applied to calibrate the HJ Model, since this method has the tendencies of getting trapped inside the suboptimal regions. To verify our speculation, we look at how the value of the

objective function (5.6) changes when we simultaneously alter the values of two model parameters. Figure 5.10 presents a three-dimensional graph of SSE surface when we concurrently change the parameter values of ρ and σ_X. As we can see, the global minimum, which is denoted by a blue dot in the graph, lies within a wide, flat valley where gradients of the objective function are nearly zero. A similar situation is seen in Figure 5.11 when we alter the parameter values of both σ_X and σ_Y. Under these circumstances, the optimization method tends to find the flat region and terminates before reaching the global minimum. This helps to explain why the estimates of $\bar{\bar{\phi}}$, ρ, σ_X, and σ_Y can take multiple possible solutions, instead of a unique solution at the global minimum.
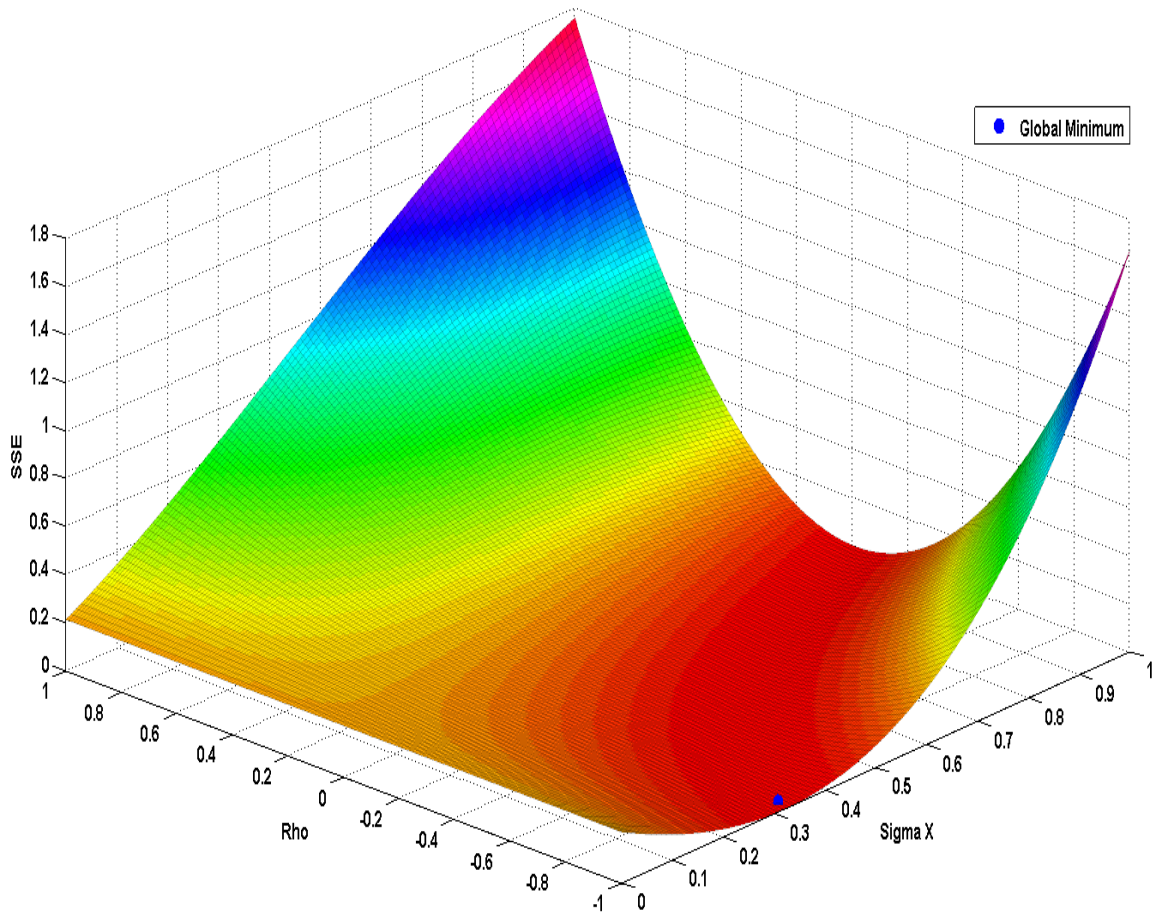

Figure 5.10 SSE surface when parameter values of ρ and σ_X are simultaneously altered
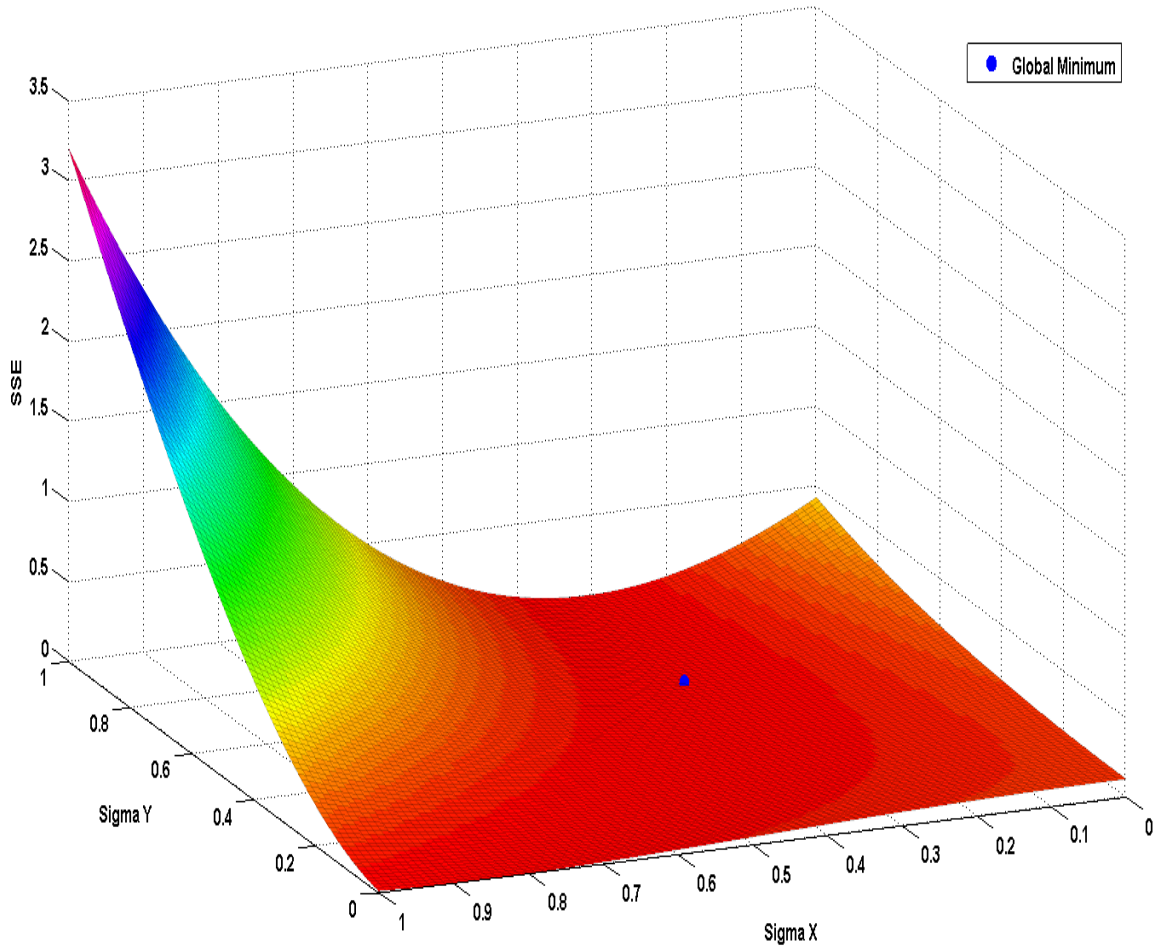
Figure 5.11 SSE surface when parameter values of σ_X and σ_Y are simultaneously altered

5.5 Model Uncertainty

As mathematical models play an increasingly important role in the valuation of derivative products, many studies have stressed the importance of "model risk" or "model uncertainty" in understanding the risk associated with derivative instruments. According to Cont (2006), model uncertainty can lead to the mispricing of derivatives and it represents a major factor of risk as significant as the market risk. This type of risk is tied to ambiguity in the choice of the model, which can be caused by the uncertainty about either the model type (for example, local volatility versus jump diffusion model) or the

specification of model parameters. Furthermore, Cont recognized that any calibration problem, which has multiple solutions, can lead to model uncertainty in the valuation of derivatives. Based on the discussion in Section 5.1, we know that the evolutions of implied market prices of risk depend on the specifications of risk-neutral model parameters. However, we obtain many possible solutions for parameters $\bar{\phi}$, ρ, σ_X, and σ_Y from the calibration process and this can cause the implied market prices of risk to have model uncertainty. Therefore, we are interested to examine how the choice of calibrated values can impact the evolutions of implied market prices of risk. To compare the evolutions of implied market prices of risk, two sets of calibrated values (Table 5.25), which have the same RSS values, are chosen to solve equations (4.17)-(4.22). The *fsolve* function in Matlab is used to solve these equations so that we can obtain the implied market prices of risk. From Figure 5.12, we observe that the implied market prices of risk, λ_t and ψ_t, which are extracted with "Parameter Set 2" are significantly larger than those obtained with "Parameter Set 1". Moreover, we also note that the processes of ψ_t for these two parameter sets will evolve differently over time. Hence, even with two sets of parameters that have the same RSS values, we will still face the problem of model uncertainty in extracting the implied market prices of risk.

	$\bar{\alpha}$	$\bar{\beta}$	$\bar{\phi}$	ρ	σ_X	σ_Y	RSS
Set 1	0.15	0.31	3.1128	-0.5171	0.4515	0.649	0.000001
Set 2	0.15	0.31	3.2705	-0.9641	0.329	0.63	0.000001

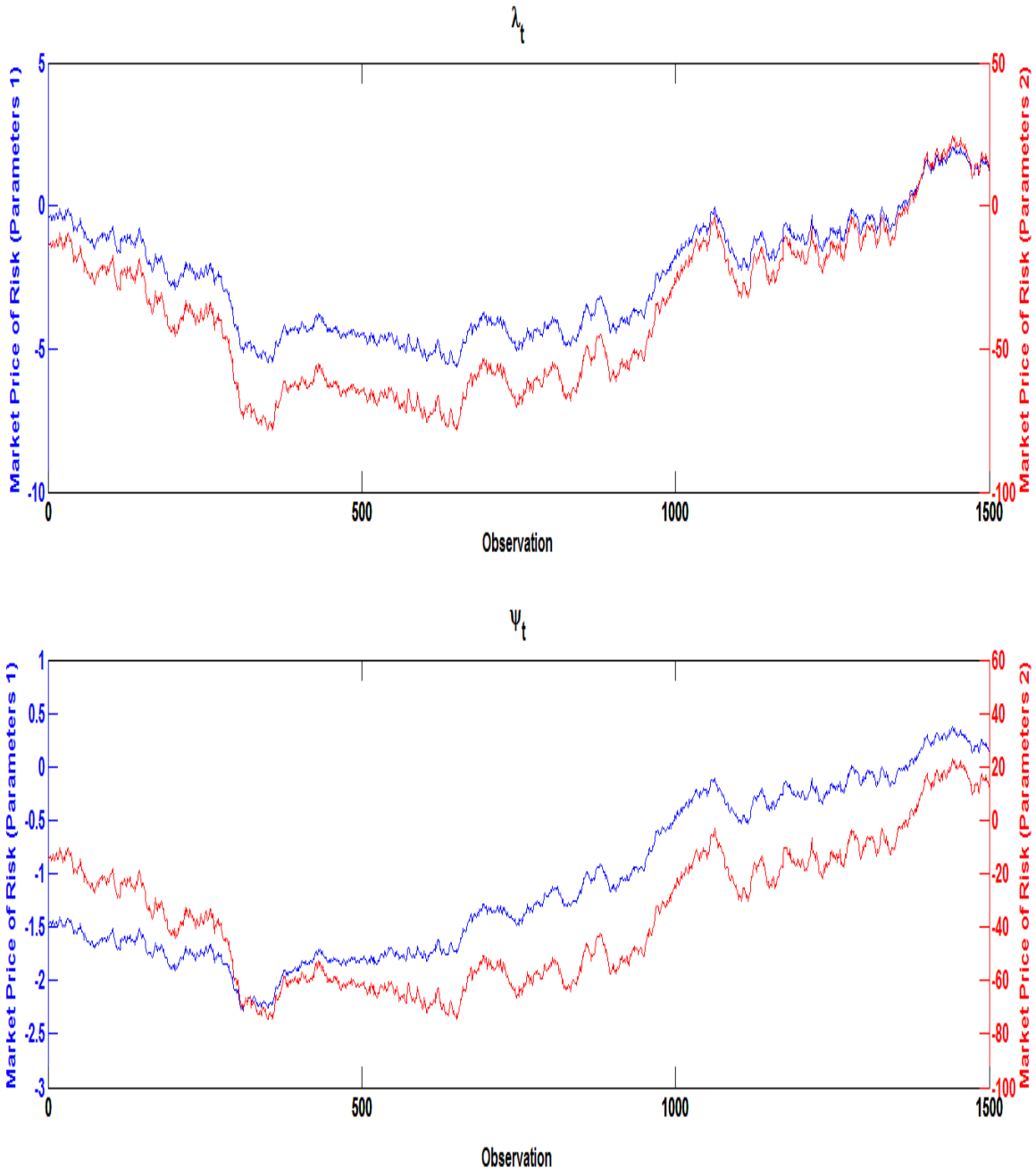Table 5.25 Parameter values used in extracting the implied market prices of risk

Figure 5.12 Market prices of risk, λ_t and ψ_t, extracted from two different parameter sets

Chapter 6

Application to Real Data

In this chapter, we present the results of calibrating the HJ Model to actual historical data of NYMEX Light Sweet Crude Oil (CL) prices. To compare our calibration results with those obtained by Hikspoors and Jaimungal, the spot and futures data used in our study are from a similar time period, 01/10/2003 to 25/07/2006, as that used in their paper. For each trading day, thirteen monthly futures contracts, with maturities from 1 month to 13 months, will be used to construct the futures curves in our analysis. The total amount of trading involving these 13 contracts represents the majority of the trading volumes in the CL market and hence these data should provide accurate price information. Figure 6.1 illustrates the evolutions of spot prices together with the 7-month and 13-month futures prices for the given time period.

We start our analysis by calibrating for the risk-neutral model parameters. With the aim of achieving a better estimation result, we use the calibrated risk-neutral parameter values obtained by the authors as the initial guesses for our optimization process. Table 6.1 presents our calibration result along with the SSE value obtained when
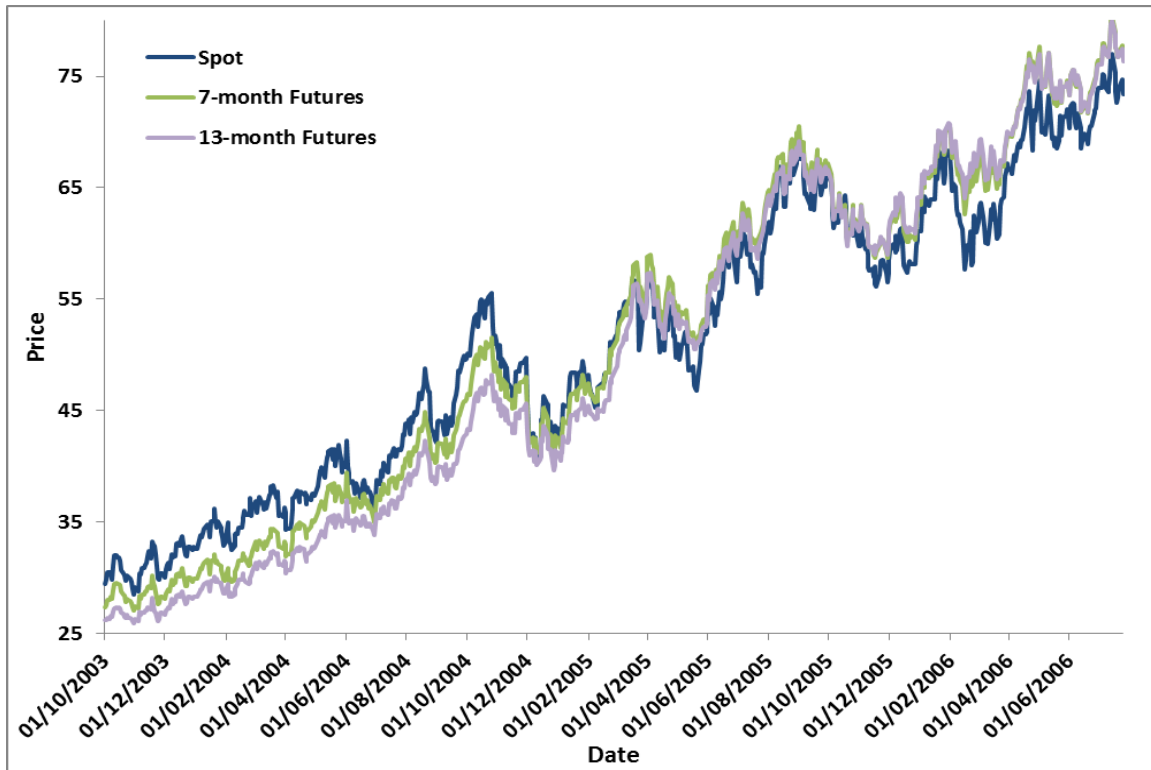
Figure 6.1 Crude oil spot and futures prices for the period 01/10/2003 to 25/07/2006

	$\bar{\alpha}$	$\bar{\beta}$	$\bar{\phi}$	ρ	σ_X	σ_Y	SSE
New	1.0037e-10	1.3322	4.0505	-0.9907	0.7459	0.1830	0.3584
HJ's	0.15	0.31	3.27	-0.96	0.33	0.63	0.6795

Table 6.1 Comparison between the SSE values acquired from our estimation result ("New") and that obtained with Hikspoors and Jaimungal's (HJ's) parameters

the HJ Model with authors' parameters is applied to our dataset. We can notice very obvious differences between our calibrated risk-neutral parameters and those provided by the authors. However, judging by the SSE values acquired from both sets of the parameters, we discover that our estimation actually provides a better fit to the dataset. We also notice from our calibration result that the estimated value of $\bar{\alpha}$, which denotes the mean-reversion rate of the stochastic mean level Y_t, is very close to zero. This might

83

suggest that the evolution of Y_t can be better described by a Brownian motion. Subsequently, we perform several linear regressions, as mentioned earlier in Section 5.1, to estimate the real-world model parameters. Table 6.2 shows the estimation results obtained for the real-world model parameters, namely α, β and ϕ.

Parameters	α	β	ϕ
Estimated Values	0.4263	1.1413	4.1854

Table 6.2 Estimated values of the real-world parameters

Since the calibration of risk-neutral model parameters involves an optimization process, we are interested in examining how various selections of initial guesses can affect estimation results. To achieve this goal, we repeat the same procedure mentioned in the previous chapter, whereby we randomly select the initial guesses of all the parameters from their respective ranges of reasonable values. Table 6.3 summarizes the calibration results obtained after performing the optimization process with 200 sets of distinctive initial guesses. From this table, we notice that the estimates of $\bar{\alpha}$, $\bar{\beta}$ and σ_Y are extremely stable with very low standard deviations among the parameter estimates obtained from various initial guesses. On the contrary, multiple possible solutions are

	$\bar{\alpha}$	$\bar{\beta}$	$\bar{\phi}$	ρ	σ_X	σ_Y	*SSE*	*Iterations*
Mean	2.3E-10	1.33221	3.82818	-0.65680	0.79859	0.18303	0.35844	44.09
Standard Deviation	3.8E-10	2.3E-05	0.36564	0.29330	0.04850	7.64E-05	3.06E-09	10.08
Minimum	1.0E-10	1.33209	3.34885	-1	0.74450	0.18293	0.35844	13
25th Percentile	1.0E-10	1.33220	3.42285	-0.88118	0.76227	0.18298	0.35844	38
75th Percentile	2.5E-10	1.33223	4.19381	-0.52592	0.81818	0.18306	0.35844	49.25
Maximum	4.8E-09	1.33224	4.34407	0.39166	0.98381	0.18339	0.35844	78

Table 6.3 Calibration results obtained from actual CL data after performing optimization with 200 distinctive sets of random initial guesses

attained for parameters $\bar{\phi}$, ρ and σ_X from the optimization process. Furthermore, we cannot easily identify which calibrated values provide the best estimates since they have all yielded the same SSE values of 0.35844. We speculate that this phenomenon is again due to the fact that the optimization algorithm fails to converge to the global minimum, after getting trapped inside an extremely flat region that surrounds the global minimum. Figure 6.2 shows the histograms of all the solutions obtained for $\bar{\phi}$, ρ and σ_X, after performing the calibration process with 200 sets of different random initial guesses.
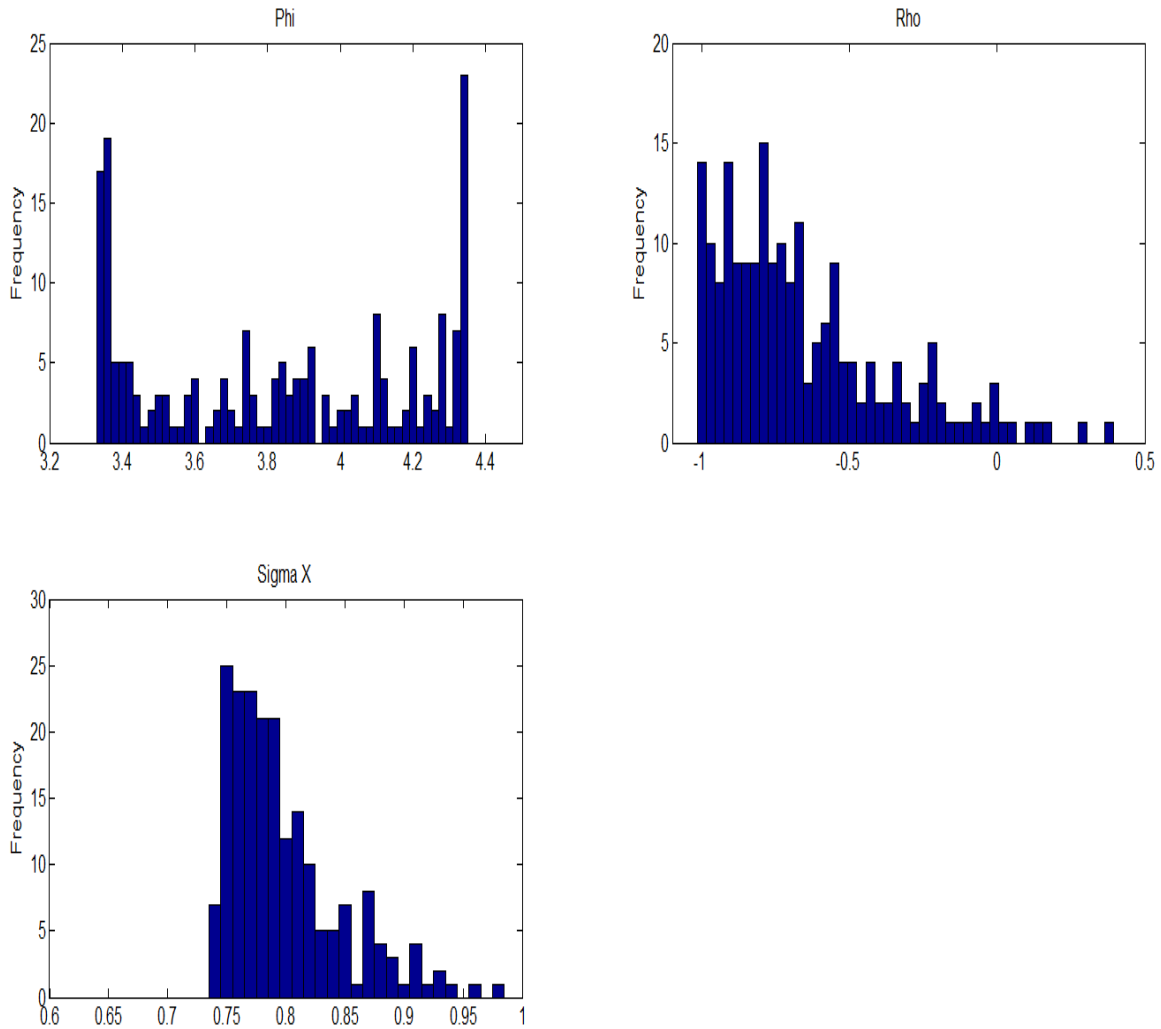

Figure 6.2 Histograms of estimated values for $\bar{\phi}$, ρ and σ_X when calibration is performed on actual CL data with 200 sets of distinctive random initial guesses

Since the calibration procedure has produced multiple possible solutions for the risk-neutral model parameters, it is natural to ask whether these results will lead to model uncertainty in the computation of implied market prices of risk. Figure 6.3 illustrates that the evolutions of implied market prices of risk can be significantly different when two distinctive sets of calibrated parameter values are used to extract the results. Hence, given that we have multiple solutions for the risk-neutral parameters, we will encounter model uncertainty in extracting the implied market prices of risk.
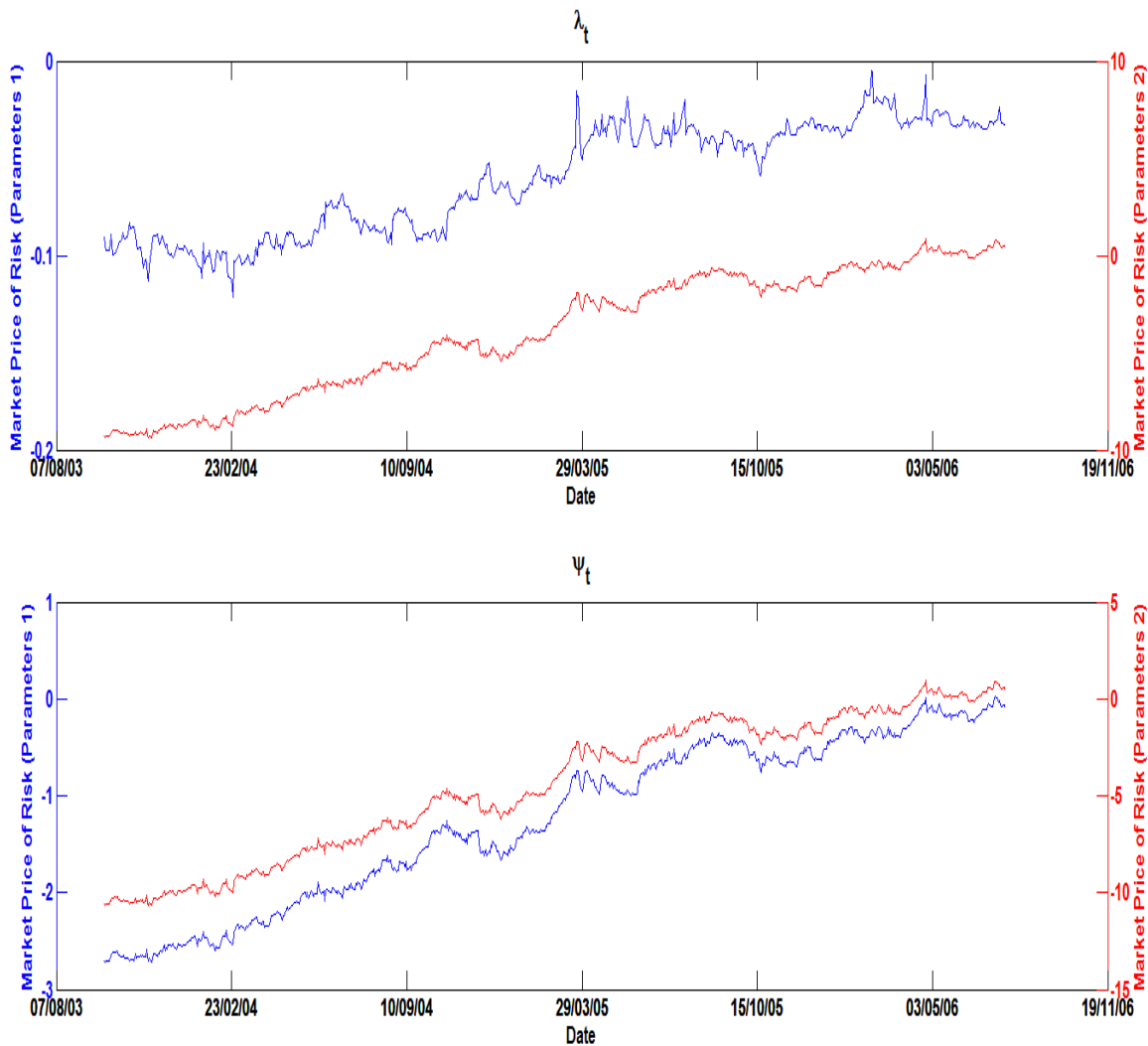

Figure 6.3 Market prices of risk, λ_t and ψ_t, for the CL market which are extracted from two different parameter sets

Chapter 7

Conclusions

In this paper, we discussed a two-factor mean-reverting stochastic model proposed by Hikspoors and Jaimungal for modelling the spot prices of commodities. Within this modeling framework, the authors successfully derived a closed-form solution for pricing futures contracts. Furthermore, they suggested a calibration method which can be used to simultaneously calibrate the risk-neutral and the real-world model parameters. By knowing the values of these parameters, one can proceed to extract the implied market prices of risk for a given commodity market. Given the usefulness of this model, we were motivated to examine the robustness of the calibration procedure to provide stable and accurate parameter estimates. Hence, we presented some of the observations and problems which we have encountered over the course of our investigation.

Based on our analysis, the calibration technique was capable of providing very stable and accurate estimates of $\bar{\alpha}$ and $\bar{\beta}$, when their initial guesses were deviated from the true values. However, a few exceptions applied when the initial guesses were set to deviate too far from the true values, which caused the optimization algorithm to find

locally optimal solutions. Meanwhile, the calibration technique had a lot of difficulties in estimating the correct parameter values of $\bar{\phi}, \rho, \sigma_X$, and σ_Y, when their initial guesses differed from the actual values. Therefore, it is interesting to note that our results do not support previous findings that the drift parameters are generally more difficult to estimate than the diffusion parameters (see, Phillips and Yu (2005) and Tang and Chen (2009)). Moreover, we detected the presence of interactions among these four parameters since the estimation of one parameter would also depend on the initial guesses of other parameters.

When the calibration procedure was performed multiple times with different sets of randomly selected initial guesses, there was an 18% chance that the estimations of $\bar{\alpha}$ and $\bar{\beta}$ failed to converge to the correct values. However, one could easily distinguish the accurate parameter estimates from the local optimums by simply comparing the SSE values obtained. On the other hand, multiple possible solutions were acquired for the estimations of $\bar{\phi}, \rho, \sigma_X$, and σ_Y. Since the SSE values attained for these estimations were relatively similar, we could hardly identify which calibrated values would provide the best parameter estimates. To analyze the cause of this problem, we considered the three-dimensional graphs of SSE surface by simultaneously altered the values of any two parameters. We noticed that the global minimum was surrounded by a wide, flat region where gradients of the objective function were nearly zero. Under these circumstances, the optimization method had the tendency of finding multiple solutions from the flat region, without proceeding further to reach the global minimum. Moreover, we illustrated that multiple solutions attained for the risk-neutral parameters would lead to model uncertainty in extracting the implied market prices of risk.

To compare our estimation results with those obtained by Hikspoors and Jaimungal, a dataset acquired from the same time period was used to perform the calibration procedure. We noticed that our calibrated risk-neutral parameters were significantly different from those provided by the authors. However, with a smaller SSE value obtained by our calibration result, we were confident that our estimation would actually provide a better fit to the dataset. Moreover, our estimation of $\bar{\alpha}$ was pretty close to zero and this might suggest that the evolution of Y_t could be better described by a Brownian motion. Hence, one would question the validity of those parameters provided by the authors and extra caution should be taken when these values were used in the valuation of a derivative. Finally, multiple possible solutions were provided for the estimations of $\bar{\phi}$, ρ and σ_X, when the calibration procedure was performed many times with different sets of randomly selected initial guesses. Hence, one would expect the presence of model uncertainty in the calculation of implied market prices of risk.

Overall, we found the lack of robustness in the calibration method proposed by Hikspoors and Jaimungal. Given that the calibration process failed to accurately estimate the values of certain parameters, namely $\bar{\phi}$, ρ and σ_X, additional steps should be taken to ensure the quality of the estimation results. Moreover, one should also be very careful with the presence of model uncertainty in the valuation of a derivative, when multiple solutions were given by the calibration method. Further work might involve the use of a global optimization method (for example, genetic algorithm) to eliminate the problems of finding locally optimal solutions by a standard local search method. In addition, a Kalman filter can be applied to calibrate the model parameters while simultaneously extracting the hidden long-run mean process Y_t.

Bibliography

Bjerksund, P. (1991) *Contingent claims evaluation when the convenience yield is stochastic: analytical results*. Working Paper, Norway School of Economics and Business Administration.

Bjork, T. (1998) *Arbitrage Theory in Continuous Time.* Oxford University Press.

Brennan, M. J. (1958) *The supply of storage*. American Economic Review, 48, pp. 50 − 72.

Chen, S., M. Insley and T. Wirjanto (2009) *The Impact of Stochastic Convenience Yield on Long-Term Forestry Investment Decisions.* Discussion Paper.

Cont, R. (2006) *Model uncertainty and its impact on the pricing of derivative instruments*. Mathematical Finance, 16 (3), pp. 519 -547.

Eydeland, A. and H. Geman (1998) *Pricing Power Derivatives*. RISK, 11 (10), pp. 71 − 73.

Fama, E. F. and K. R. French (1987) *Commodity futures prices: Some evidence on forecast power, premiums and the theory of storage*. Journal of Business, 60, pp. 55 − 73.

Frenkel, J. A. (1977) *The Forward Exchange Rate, Expectations, and the Demand for Money: The German Hyperinflation*. The American Economic Review, 67 (4), pp. 653 − 670.

Gabillon, J. (1991) *The Term Structure of Oil Futures Prices*. Working Paper 17, Oxford Institute for Energy Studies.

Geman, H. (2005) *Commodities and Commodity Derivatives: Modelling and Pricing for Agriculturals, Metals and Energy.* John Wiley & Sons.

Geman, H. and V. N. Nguyen (2005) *Soybean inventory and forward curves dynamics*. Management Science, 51, pp. 1076 – 1091.

Gibson, R. and E. S. Schwartz (1990) *Stochastic convenience yield and the pricing of oil contingent claims*. Journal of Finance, 45 (3), pp. 959 – 976.

Gorton, G. and K.G. Rouwenhorst (2005) *Facts and Fantasies about Commodity Futures*. Working Paper No. 04-20, Yale International Center for Finance.

Grossman, S. J. (1977) *The existence of futures markets, noisy rational expectations and informational externalities*. Review of Economic Studies, 44, pp. 431-449.

Heston, S. L. (1993) *A Closed-Form Solution for Options with Stochastic Volatility with Applications to Bond and Currency Options*. Review of Financial Studies, 6 (2), pp. 327 – 343.

Hicks, J. R. (1939) *Value and Capital*. Oxford University Press, Cambridge.

Hikspoors, S. and S. Jaimungal (2008) *Asymptotic Pricing of Commodity Derivatives Using Stochastic Volatility Spot Models*. Applied Mathematical Finance, 15 (5), pp. 449 – 477.

Hikspoors, S. and S. Jaimungal (2007) *Energy Spot Price Models and Spread Options Pricing*. International Journal of Theoretical and Applied Finance, 10 (7), pp. 1111 – 1135.

Hull, J. (2005) *Options, Futures and Other Derivatives*. 6th edition, Prentice Hall.

Jamshidian, F. and M. Fein (1990) *Closed-form solutions for oil futures and European options in the Gibson-Schwartz model: A note*. Working Paper, Merrill Lynch Capital Markets.

Kaldor, N. (1939) *Speculation and economic stability*. The Review of Economic Studies, 7, pp. 1-27.

Keynes, J. M. (1930) *A Treatise on Money*. Macmillan & Co., London, 2.

Lucas, R. E. (1976) *Econometric Policy Evaluation: A Critique*. Journal of Monetary Economics (Supp.), 1, pp. 19 – 46.

Merton, R. C. (1976) *Option Pricing When Underlying Stock Returns are Discontinuous*. Journal of Financial Economics, 3, pp. 125 – 144.

Muth, J. F. (1961) *Rational Expectations and the Theory of Price Movements*. Econometrica, 29 (3), pp. 315-335.

Phillips, P. C. and J. Yu (2005) *Jackknifing bond option prices*. Review of Financial Studies, 18, pp. 707 – 742.

Pilipovic, D. (1997) *Energy Risk: Valuing and Managing Energy Derivatives*. McGraw-Hill.

Richter, M. C. and C. Sorensen (2002) *Stochastic Volatility and Seasonality in Commodity Futures and Options: The Case of Soybeans*. Working Paper, Copenhagen Business School.

Ross, S. (1976) *The arbitrage theory of capital asset pricing*. Journal of Economic Theory, 13 (3), pp. 341 – 360.

Routledge, B. R., D. J. Seppi and C. S. Spatt (2000) *Equilibrium forward curve for commodities*. Journal of Finance, 55 (3), pp 1297 – 1338.

Samuelson, P. A. (1965) *Proof that properly anticipated prices fluctuate randomly*. Industrial Management Review, 6, pp. 41 – 49.

Samuelson, P. A. (1965) *Rational Theory of Warrant Pricing*. Industrial Management Review, 6, pp. 13 – 31.

Schwartz, E. S. (1997) *The Stochastic Behavior of Commodity Prices: Implications for Valuation and Hedging*. Journal of Finance, 52 (3), pp. 923 – 973.

Tang, C. Y. and S. X. Chen (2009) *Parameter estimation and bias correction for diffusion processes*. Journal of Econometrics, 149, pp. 65 -81.

Telser, L. G. (1958) *Futures trading and the storage of cotton and wheat*. Journal of Political Economy, 66, pp. 233 – 255.

Vasicek, O. (1977) *An equilibrium characterization of the term structure*. Journal of Financial Economics, 5 (2), pp. 177 - 188.

Working, H. (1948) *Theory of the inverse carrying charge in Futures markets*. Journal Farm Economics, 30, pp. 1 – 28.

Working, H. (1949) *The theory of the price of storage*. American Economic Review, 39, pp. 1254 - 1262.